Thermocable

Photovoltaic Array Overheat & Fire Detection

A Research Report on Linear Heat Detection Systems for Overheat and Fire Warning in Photovoltaic Applications

July 2025

ProReact

This report presents findings from world-leading research into the early detection of fire hazards in solar installations, focusing on the use of Linear Heat Detection (LHD) technologies.

Commissioned By:
Spike Armstrong, Business Development Manager, Thermocable Ltd.

Prepared By:
Slovenian National Building and Civil Engineering Institute, Section for Fire Research and Innovation

Report No. 366/25-560-1-EN

ZAVOD ZA GRADBENIŠTVO SLOVENIJE

SLOVENIAN NATIONAL BUILDING AND CIVIL ENGINEERING INSTITUTE

Dimičeva ulica 12
1000 Ljubljana
Slovenija

info@zag.si
www.zag.si

DEPARTMENT FOR FIRE-SAFE SUSTAINABLE BUILT ENVIRONMENT

Section for Fire Research and Innovation

REPORT
366/25-560-1-EN

About using Linear Heat Detection systems in PV-related fires

Orderer:	**Thermocable Flexible Elements Ltd** **Pasture Lane, Clayton** **Bradford (GB-BD14 6LU) (Great Britain)**
Order/contract:	**10235/25**
Responsible Investigator:	**Kirils Simakovs, MSc.**
Head of Laboratory/Section:	**ddr. Aleš Jug, univ. dipl. oec., var. inž.**
Director:	**doc. dr. Aleš Žnidarič, univ. dipl. inž. grad.**
Date:	25. 7. 2025

Digitalno podpisano:
ALJOŠA ŠAJNA, ZAG

(po pooblastilu direktorja)

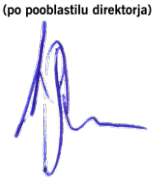

The report has been internally reviewed and approved by all listed persons, which is confirmed by the final electronic signature.
Document authenticity check : www.zag.si/pristnost

The results of the tests refer only to the tested specimens. This report may only be reproduced as a whole.
Complaints will be considered only if received within 15 days from the date of issue of the report.
Total number of pages: 48; total number of annexes : 0.

Table of content

Summary:

- After ignition of the rooftop photovoltaic (PV) system sample installed with linear heat detection system (LHD), the fire spread beneath the PV modules in all four tests, which means that there was a spread below the PV modules in all the different settings (mid-scale flat sample, mid-scale inclined sample and large-scale sample)
- Surface temperatures on the PV modules exceeded 600 °C in some cases (e.g., LHD-1), while temperatures inside the roof buildup, near its surface, at the time of alarm typically ranged between 70 °C and 270 °C, depending on ignition type and cable location
- The type of ignition influenced the initial stages of the fire development. As expected, wood crib fires caused faster, and more intense initial flame spread, while arc ignition resulted in slower initial fire development and lower peak temperatures as recorded with thermocouples at various locations
- Detection performance varied across cable types and placements
    - The fastest LHD alarm responses were observed with 88N (11 seconds) for the wood crib-ignited flat roof (LHD-1)
    - The 100+SS detected the fire in 37 seconds for the arc-ignited flat roof (LHD-2)
    - The EN88 detected the fire in 1 min and 47 seconds for the arc-ignited pitched roof (LHD-3)
    - Multiple alarms responded in under one minute, particularly during the flat roof tests (EN88, 105N, 100+SS and AN for LHD-1 and 88N, EN88, EN88SS and 105N for LHD-2), indicating strong early detection performance in those scenarios, all of which had the fastest response in ‘long’ configuration
- In the large-scale arc-ignited roof (LHD-4), the response times were longer (ranging from 3 minutes and 43 seconds to 8 minutes and 42 seconds), with EN88SS in Q1 activating first. Note that the placement of the detectors varied, compared to other tests
- Roof slope and cable routing affected alarm timing. In the pitched sample (LHD-3), detection was faster for cables placed near the top edge – ‘short’ configuration
- Although stainless-steel braided cables (e.g. EN88SS, ANSS) are designed for higher mechanical and environmental resistance due to their stainless-steel braiding over LSZH or PVC base coats, they generally exhibited delayed detection in LHD-1, where the ignition source (wood crib) was directly beneath the cable. By contrast, the 100+SS cable, which also features a stainless-steel braid but uses an LSZH base coat, demonstrated early activation in this same test. Furthermore, in LHD-2 and LHD-3, where the ignition source (an arc) was offset from the cable, the stainless-steel braided cables did not show delayed response. In fact, EN88SS (in LHD-2) exhibited some of the fastest activation times, performing comparably to or even better than their non-stainless-steel counterparts
- The results suggest that LHD systems can support early warning detection of a PV-related fire, if the cable type, placement, and fire scenario are carefully matched, thus emphasizing the need for tailored, scenario-specific design rather than standard layouts

1. Introduction

The right combination of roofing and PV system products and materials, their thickness, arrangement, and consideration of their properties under different conditions are crucial for minimising the consequences in the event of a fire.

ZAG conducted a series of tests to evaluate the effectiveness of linear heat detection (LHD) systems when a fire starts on a roof with an installed PV system.

Various methods were utilised to assess the extent of impact/damage in the tests:

- Visual inspection of the test by observing the behaviour of the fire and various parts of the system
- Video recordings from different angles
- Measurement of the temperature (measured with thermocouples (TCs) placed on different layers of the roof structure during and after the test)
- Measurements of the linear heat detection system
- Visual inspection of the damage to the PV system and the underlying materials (depth and extent) was assessed after the end of the test

The results of the tests are analysed to better understand the effectiveness of the LHD systems during the initial stages of fire spread under the PV module.

Details on ZAG`s test method can be provided on request.

2. Test matrix, design and execution

2.1 Test matrix

The specimens were built according to Table 1. The combination of materials used in the roof part of the specimens represents some of the more common roof buildups.

Table 1 Test matrix for the 4 specimens

Mid-scale specimen, (2.5 × 2.5) m			**Large-scale specimen, (4 × 3.5) m**
LHD-1	**LHD-2**	**LHD-3**	**LHD-4**
Flat		20-degree slope	No slope
Wood crib	Arc	Arc	Arc ignition
JinKo Solar JKM450N-54HL4R-V		Panel vision GM 3.0	Jinko Solar Tiger Neo JKM440N-54HL4R-V
S-Dome 6.15 (15 degrees)	PMT EVO 2.1 (15 degrees)	K2 SingleRail System	D-Dome 6.15 with S components (15 degrees)
PVC Sikaplan G-18 (1.8 mm)			
-		OSB boards (12 mm)	-
Rockwool Hardrock Max (50 mm)			
Fragmat EPS 150 W30 (150 mm)			

2.2 Specimen design and assembly process

The schematics of the mid-scale and large-scale specimens are shown in Figure 1. The top row shows a schematic of a mid-scale flat sample (top-left) and a mid-scale pitched sample (top-right), and the bottom row shows a schematic of a large-scale flat roof sample. Orange lines highlight the locations of LHD components.

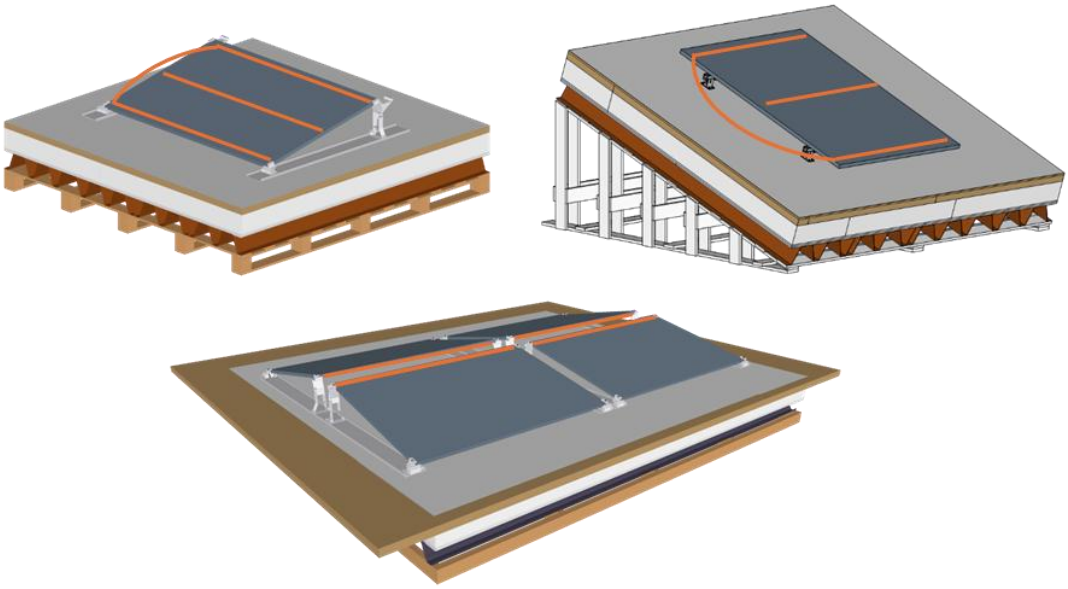

Figure 1 Mid-scale (top) and large-scale (bottom) specimen illustrations with LHD positions depicted in orange

The cross-sections of the structure of the samples are shown in Figure 2.

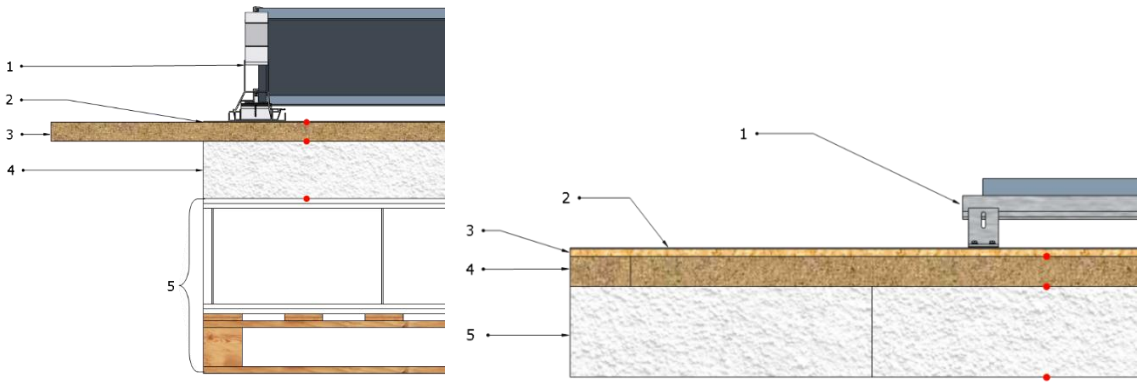

Figure 2 Specimen cross-section (side-view) for flat roofs (left) and pitched roofs (right)

1. PV system
2. Roof membrane
3. Mineral wool (on the left) and OSB board (on the right)
4. EPS (on the left) and mineral wool (on the right)
5. Roof substrate (on the left) and EPS (on the right)

2.3 Linear Heat Detection (LHD) specimen installations

The linear heat detection (LHD) systems were installed by the client, using standardised layouts for both digital and analogue configurations. The installations were designed to evaluate how detection performance varies with cable type, routing geometry, and test scale. Three installation setups were used: mid-scale analogue (Figure 3), mid-scale digital (Figure 4), and a large-scale mixed analogue/digital setup (Figure 5).

For the mid-scale **digital** setup, each test panel included two detection zones using the same digital LHD cable, resulting in ten digital zones per panel. Two cable routing strategies were used: a long run, which passed twice over the panel approximately 100 mm from the top and bottom edges (total length 17 m), and a short run, which passed once down the centre of the panel (7 m). Each cable run was connected to a dual-zone digital controller - either a digital sensor control until (DSCU) or dual in-line memory module (DiMM) unit - and terminated with either a 3.6 kΩ (DSCU) or 1 kΩ (DiMM) resistor. Digital systems had no minimum required cable length.

In the mid-scale **analogue** setup, each panel contained two analogue detection zones, resulting in four analogue zones per panel. The same long and short routing configurations were used (17 m and 7 m, respectively), but due to the minimum 50 m cable requirement for analogue systems, additional coiled lengths were added: 33 m to the end of each long run and 43 m to each short run. These cables were connected to single-zone Analogue Composite Control Units (ACCU) and terminated using analogue end-of-line (EOL) modules.

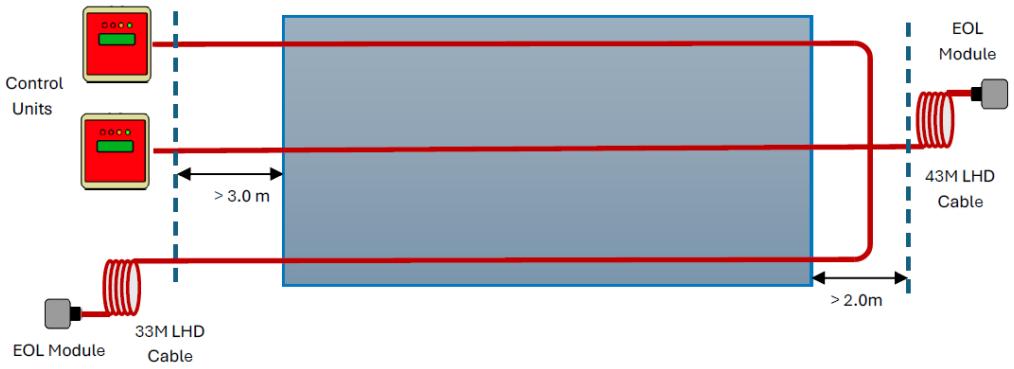

Figure 3 Analogue LHD system design (mid-scale)

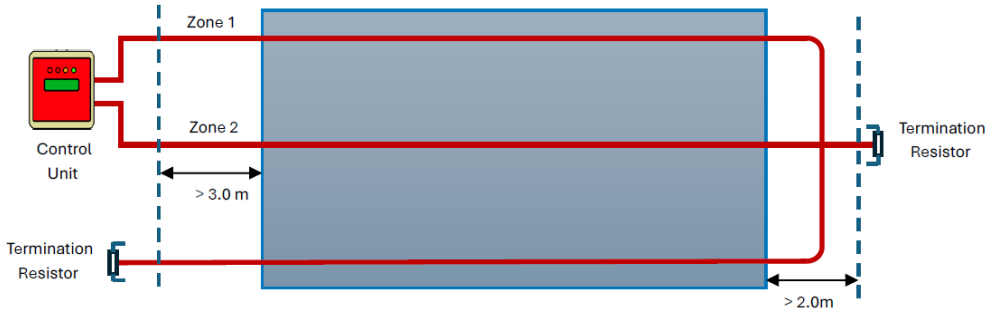

Figure 4 Digital LHD system design (mid-scale)

The large-scale installation combined both digital and analogue systems. Each panel was fitted with two digital zones and one analogue zone, giving a total of three zones per panel. In this setup, each zone was assigned to a single panel, with the specimen divided into four separate zones (Q1-4). This arrangement enabled assessment of how quickly a given LHD configuration would respond when the fire originated on an adjacent panel. All cable runs used the short configuration, passing once along the top of each panel with an approximate length of 7 m.

In total, seven LHD cable variants were tested: five digital and two analog. These included differences in base material (PVC or Low Smoke Zero Halogen), jacket type (nylon or stainless-steel braid), and compatibility with the respective digital or analogue systems. A summary of cable constructions and control units is provided in Table 2.

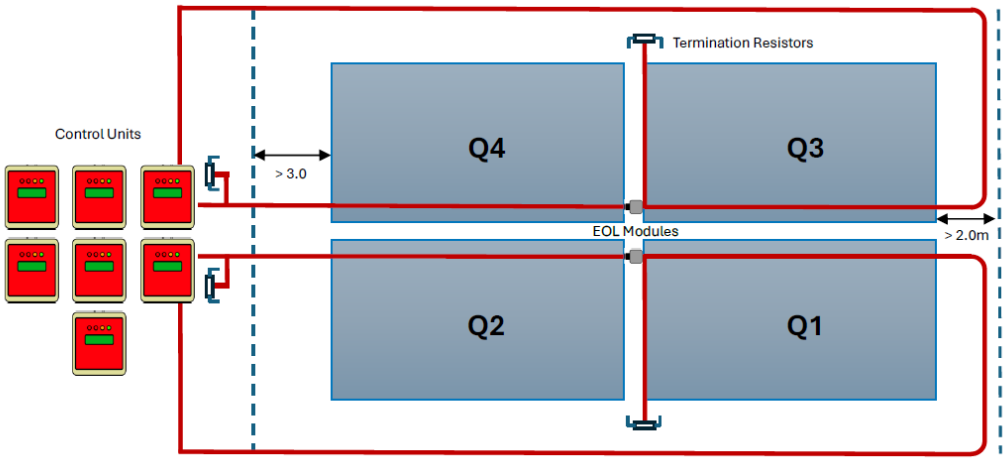

Figure 5 Digital and Analogue LHD system design (large-scale)

Table 2 Overview of tested LHD cable variants

System	Control Unit	Serial No.	Zone	Part Code	LHD Cable Description	Meters
1	ProReact Digital DiMM*	1081478	1	F1072	ProReact Digital 88 PVC Nylon	17
			2			7
2	ProReact Digital DiMM	1081481	1	F1073	ProReact Digital 105 PVC Nylon	17
			2			7
3	ProReact Digital DiMM	1081480	1	F1131	ProReact Plus Digital 100 LSZH SS	17
			2			7
4	ProReact EN DSCU**	1080856	1	F1181	ProReact EN Digital EN88 LSZH	17
			2			7
5	ProReact EN DSCU	1080925	1	F1191	ProReact EN Digital EN88 LSZH SS	17
			2			7
6	ProReact EN ACCU***	1082754	Short	F3052	ProReact EN Analogue PVC SS	50
	ProReact EN ACCU	1084140	Long	F3051	ProReact EN Analogue PVC Nylon	50
7	ProReact EN ACCU	1084159	Long	F3052	ProReact EN Analogue PVC SS	50
	ProReact EN ACCU	1084145	Short	F3051	ProReact EN Analogue PVC Nylon	50

* - Digital Interface Monitor Module

** - Digital Sensor Control Unit

*** - Analogue Composite Control Unit

2.4 Event logging, temperature measurements, ignition source and test procedure

A timeline of all observed events and phenomena during the flaming phase of each experiment was compiled to provide a comprehensive overview of the process (see section 3.1). Cameras from different angles were also used to record videos of the experiments.

To assess the extent of the damage, photo and video footage were used throughout the flaming phase and during dismantling of the specimens to document the condition of the linear heat detection system, PV modules, mounting system and roofing materials.

Various linear heat detection cables were utilised to compare the extent of the fire at the time of detection.

K-type shielded thermocouples (TCs) were used to measure the temperature development inside the roof segments and at some locations on/under the PV modules. TCs in the roof segments were placed at various depths to assess the penetration of heat by the fire and the effects of it on the roof materials during and after combustion.

The placement of thermocouples between materials is indicated with red dots in Figure 6, Figure 7, Figure 9, Figure 11 and Figure 12. The numbering system for the thermocouples is shown in Figure 8, Figure 10 and Figure 13.

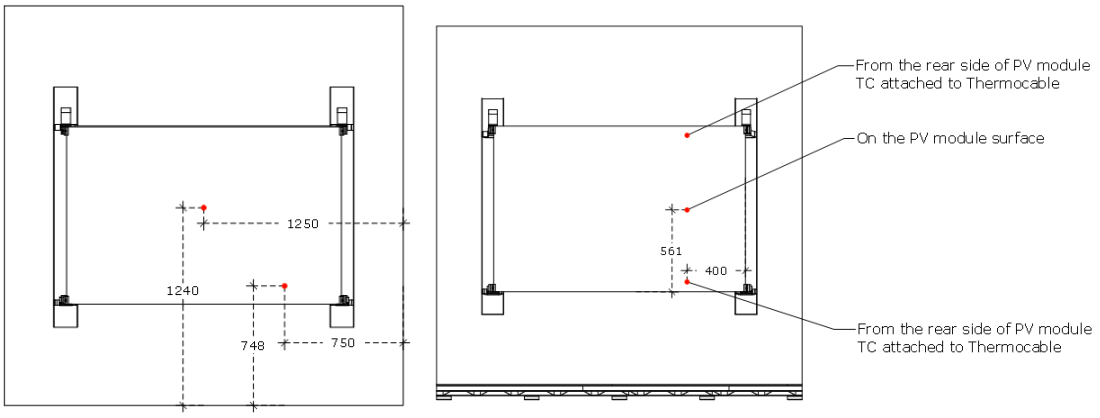

Figure 6 Locations of TCs on mid-scale flat-roof specimens (LHD-1): inside the roof (left) and on/under PV module (right)

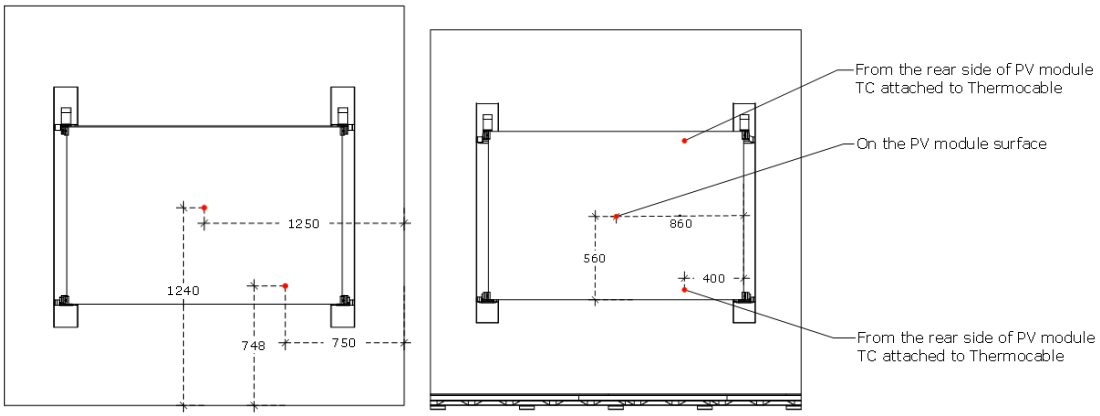

Figure 7 Locations of TCs on mid-scale flat-roof specimens (LHD-2): inside the roof (left) and on/under PV module (right)

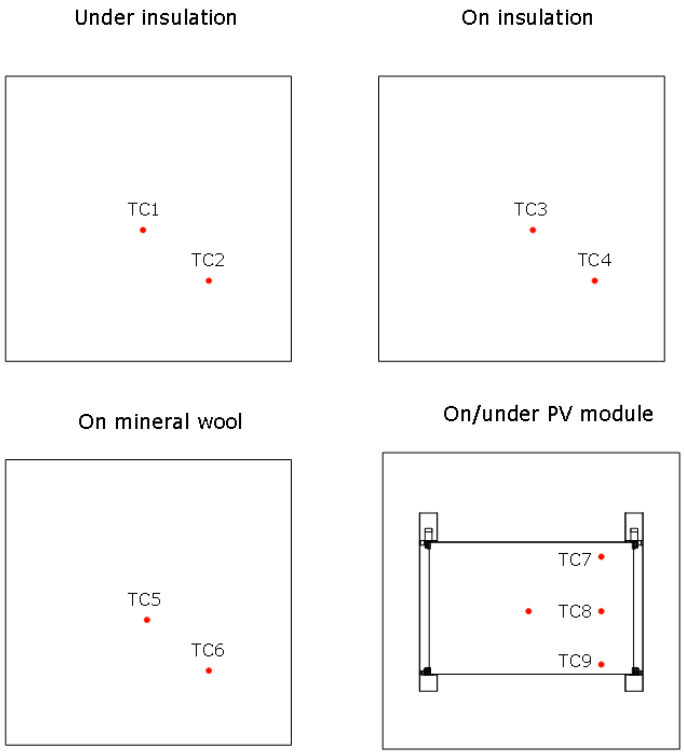

Figure 8 Numeration of TCs at the flat roof mid-scale specimens (LHD-1 and LHD-2)

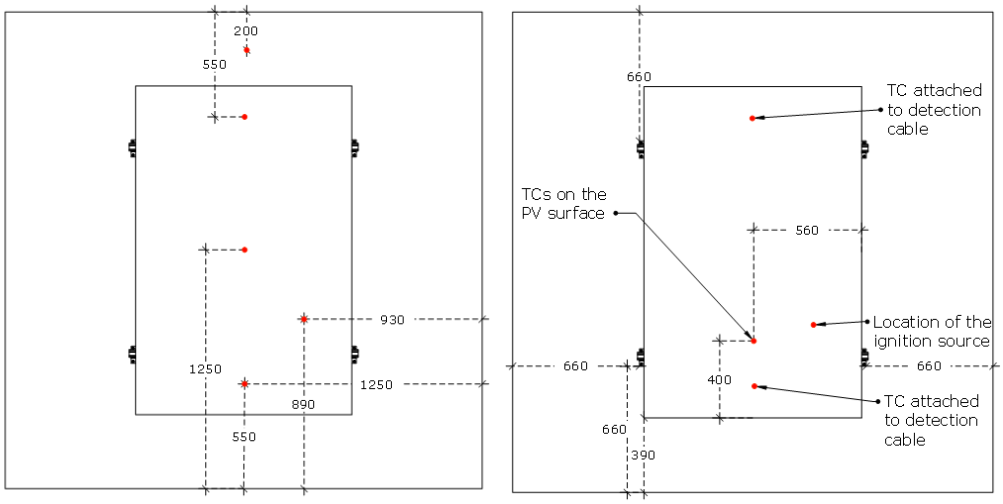

Figure 9 Locations of TCs on mid-scale pitched-roof specimen (LHD-3): inside the roof (left) and on/under PV panel (right)

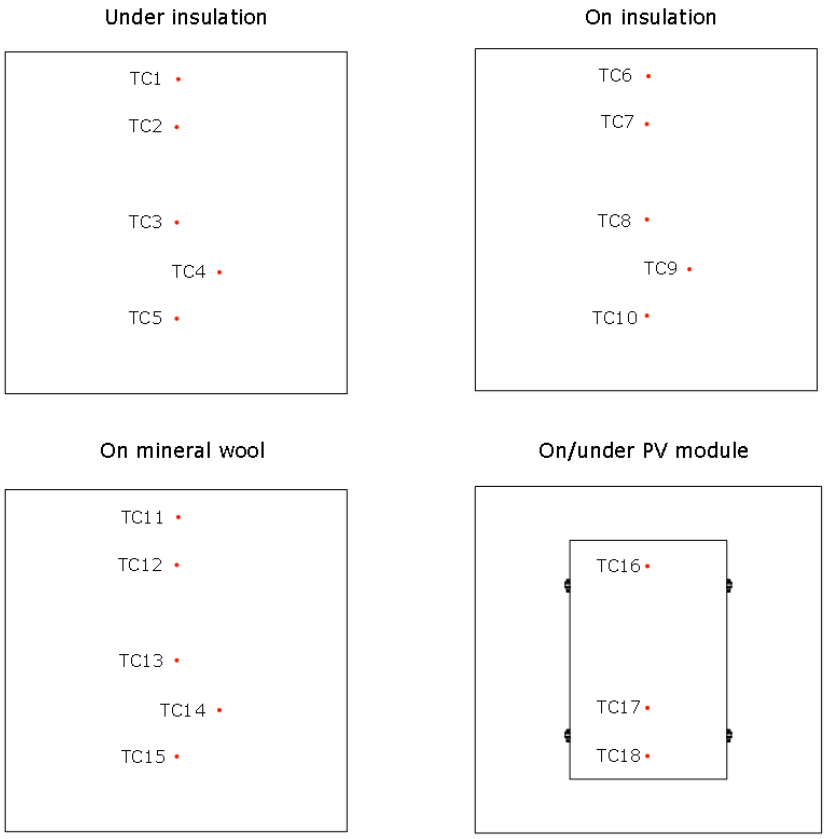

Figure 10 Numeration of TCs at the pitched roof mid-scale test (LHD-3)

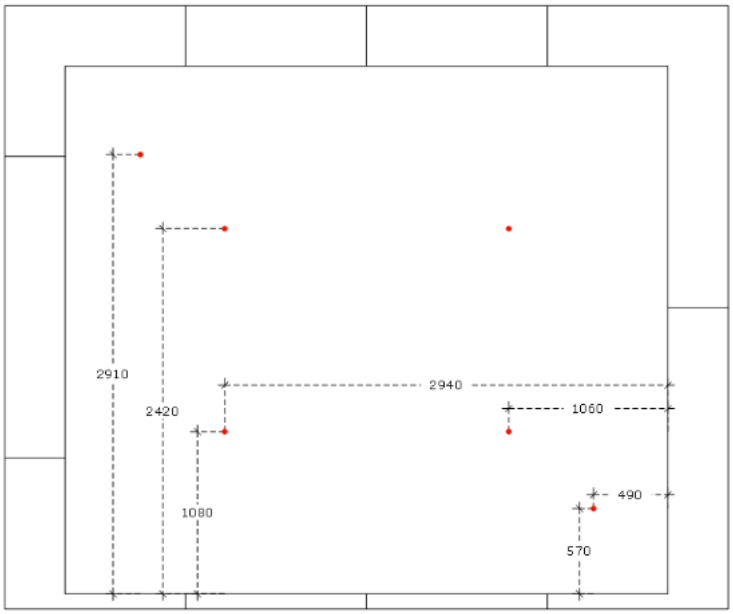

Figure 11 Locations of TCs on the large-scale specimen (LHD-4): inside the roof

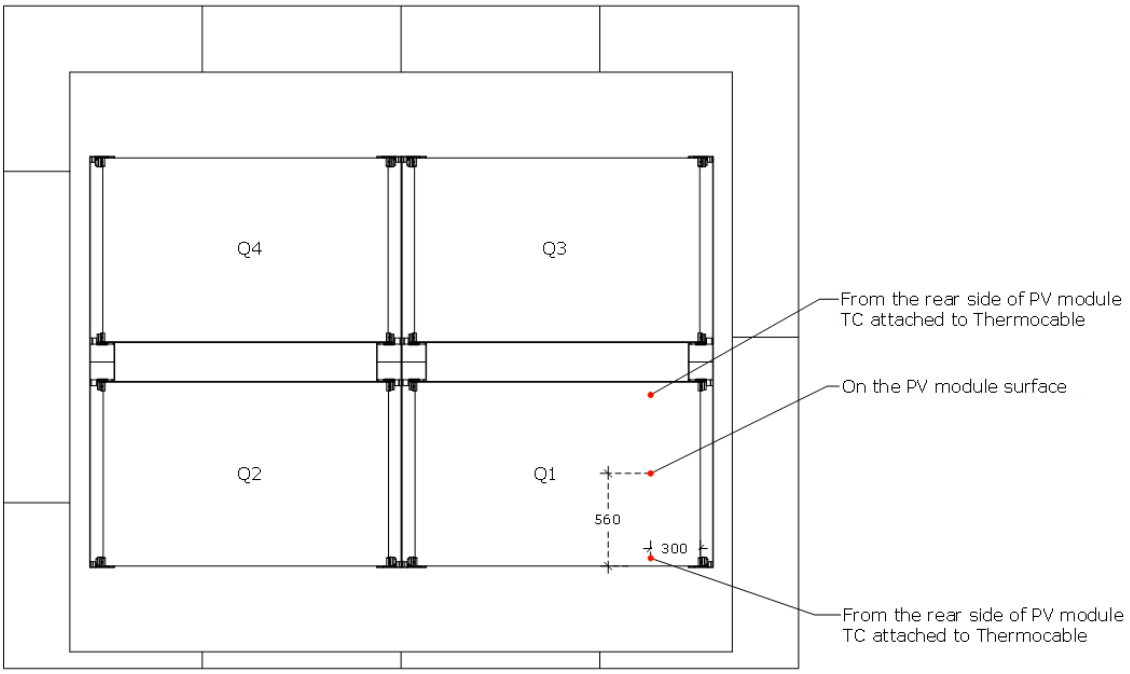

Figure 12 Locations of TCs on the large-scale specimen (LHD-4): on/under PV module

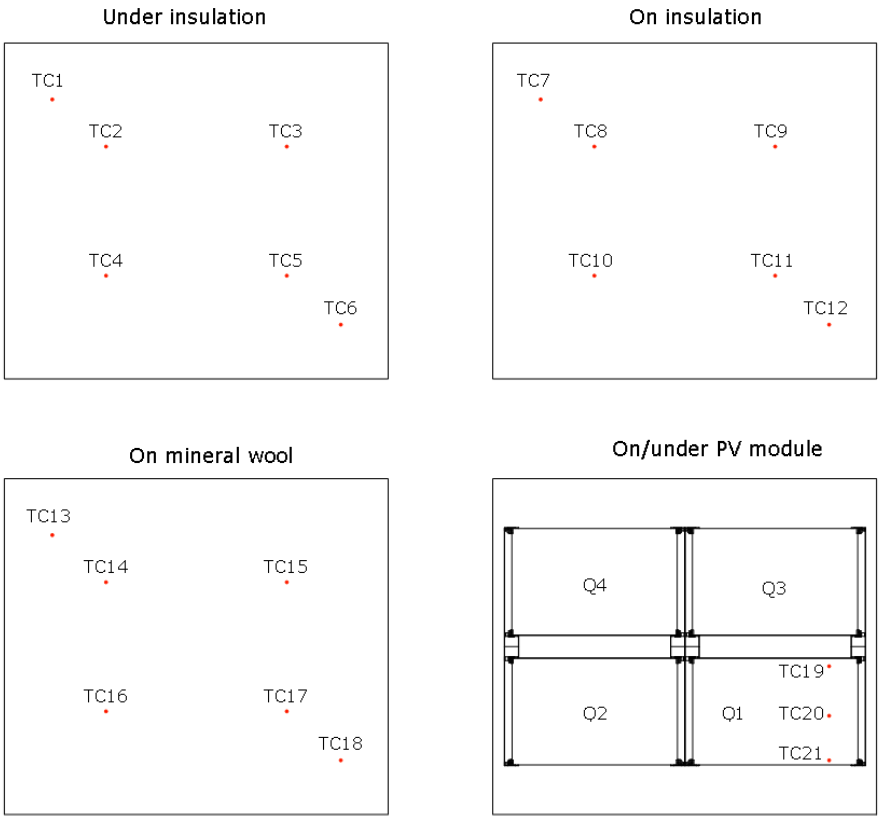

Figure 13 Numeration of TCs on a large-scale test (LHD-4)

2.5 Ignition source

For the ignition of the tests, two different ignition sources were utilised – a wood crib and an electric arc formed with a PV connector.

Schematic of the used ignition source – wood crib – is shown in Figure 14.

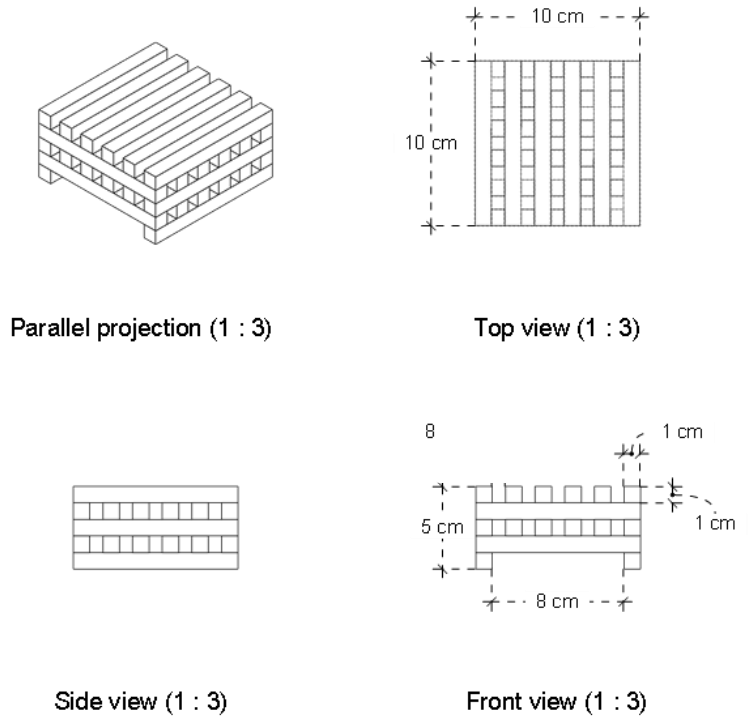

Figure 14 Illustration of the wood crib

An arc generated by moving the DC connector was utilised to mimic the scenarios of a connector fault. An illustration of a connector holder device for manual arc generation is shown in Figure 15.

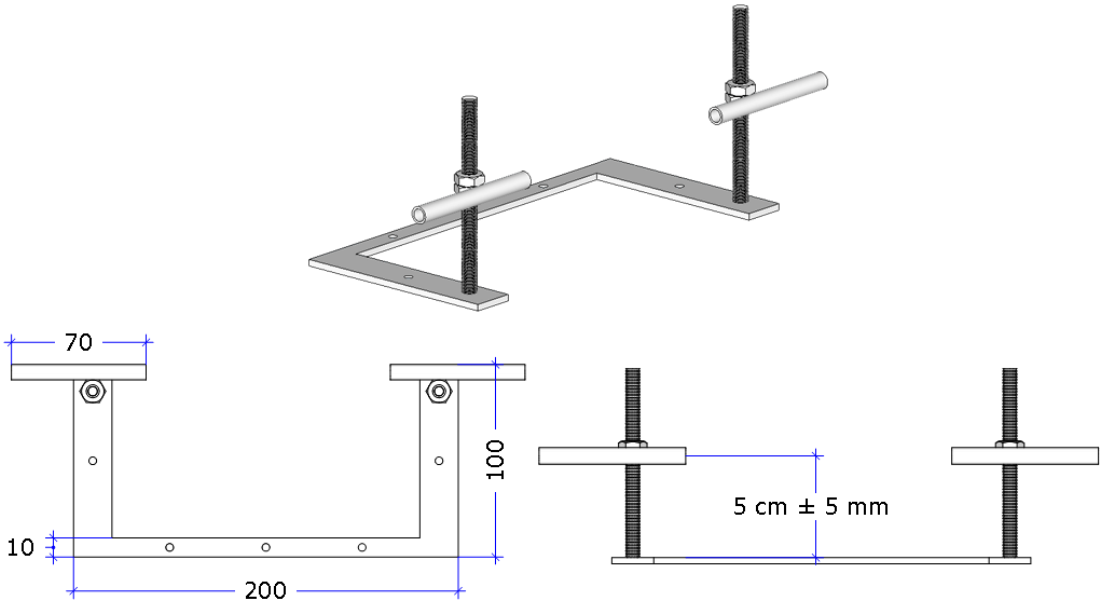

Figure 15 Connector jig

2.6 Test procedure

The following steps outline the general experimental procedure.

2.6.1 Ignition with a wood crib

- Dried wood crib is soaked in ≈6 mL of isopropyl alcohol and placed under the PV module in the defined position (section 2.4).
- The crib is ignited with a lighter.
- The detection time with LHD was noted.
- The test was continued until the entire area under the PV module was involved in the fire.

2.6.2 Ignition with an electric arc

- Connector holder with the cables and Staubli MC4 connectors placed in the position defined in the section 2.4.
- A welding machine was utilised as a power source for arc generation.
- Current was set at 45A.
- Connectors were moved back and forth until an arc appeared and ignited a roof membrane
- The detection time with LHD was noted.
- The test was stopped based on visual observations and in consultation with the client.

3. Results

3.1 Observations during and after the tests

The following subchapters represent a collection of all the observations made during and after the tests. They come from technicians who observed the tests, from photos of the observed phenomena and from snapshots from videos taken by the cameras. The visual material is accompanied by commentaries explaining the events depicted in more detail.

3.1.1 LHD-1

Date and time of test: 2025.06.15, 14:24.

Temperature/Relative humidity: 21 °C / 41%.

The documented observations and events of the LHD-1 test are summarised in Table 3. The most important events are illustrated by photos and video screenshots taken at times during the test when the detection system was triggered.

Table 3 Observations for test LHD-1

Time (min)	Events
1	Detection cables are involved in the fire
3	Delamination of PV cells was observed
4	Flames went out from the top and right side
4.5	Detection cable located at the top edge released volatile compounds that ignited, creating a» jet flame« effect. Flames were coloured blue and green due to the presence of various chemical components in the structure of the LHD cable.
5	LHD cable transfers the flames
8.5	Fire reached the end of the left side of the specimen
14	Fire slows down. Most of the flames are on the right side of the specimen.
17	The glass of the PV panel broke.
22.5	No more flames on the roof.

The fire involved detection cables within the first minutes of the test (Figure 13). Delamination of the PV cells in the PV module was observed by minute 3, followed shortly by flames emerging from the top and right sides of the PV module. Around 4.5 min after ignition, detection cables located near the top edge of the specimen released volatile compounds that ignited, producing a distinct jet flame effect with blue and green flames, attributed to the presence of the various chemical components present in the LHD cables. Due to the characteristics of these flames, capturing them on camera was difficult with the available cameras. By minute 8.5, the fire had spread to the far-left edge of the specimen. The intensity of the fire began to decrease after minute 14 and was mainly located on the right side of the sample. At 17 min, the glass of the PV panel broke as shown in Figure 14. No more flames were observed on the roof surface after 22.5 min.

Figure 16 Detection cables on fire 1 min (left) and 6 min (right) after the ignition (FotoPortal (left 050522d-001, right 050522d-002))

Figure 17 Specimen towards the end of the test (FotoPortal 050522d-003)

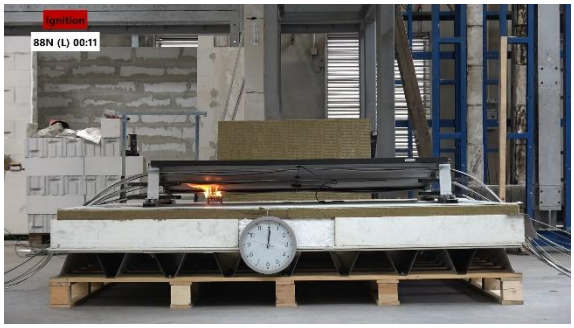

0:11 – 88N (L)

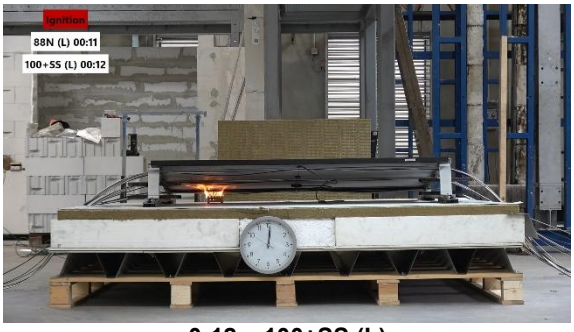

0:12 – 100+SS (L)

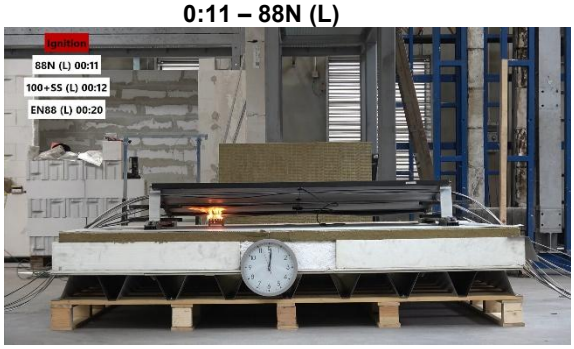

0:20 – EN88 (L)

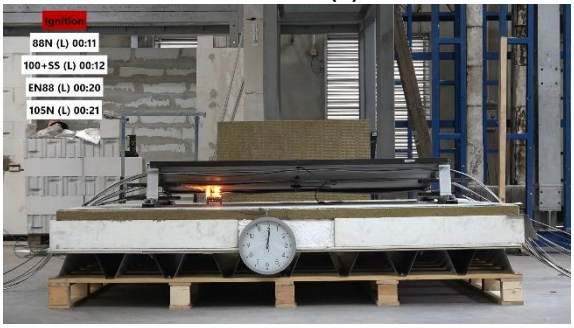

0:21 – 105N (L)

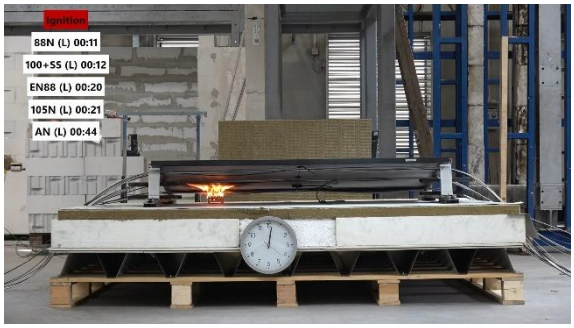

0:44 – AN (L)

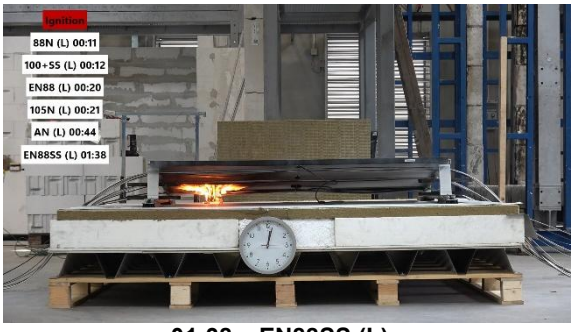

01:38 – EN88SS (L)

01:44 – ANSS (L)

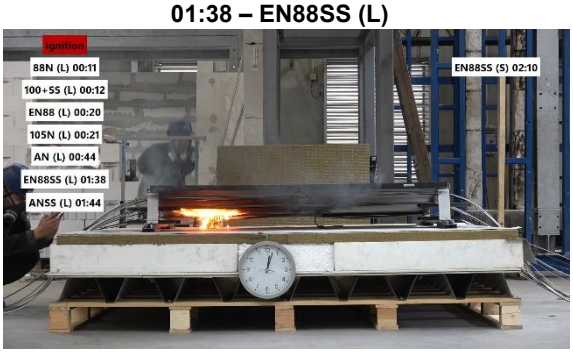

02:10 – EN88SS (S)

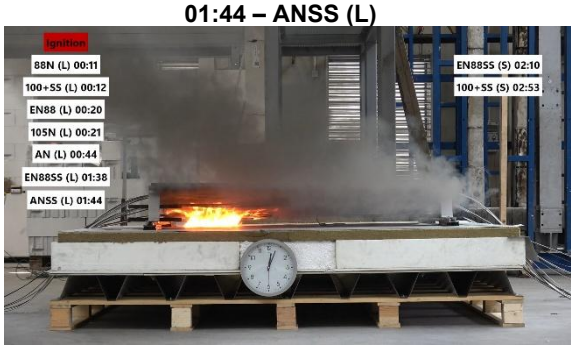

02:53 – 100+SS (S)

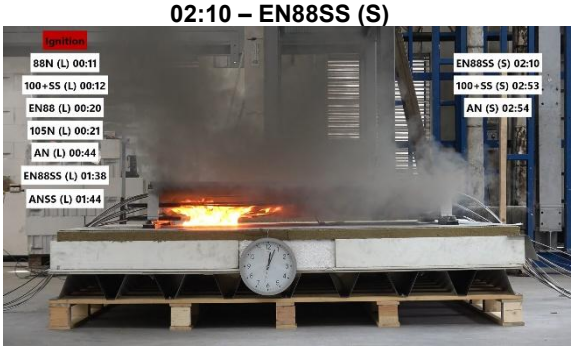

02:54 – AN (S)

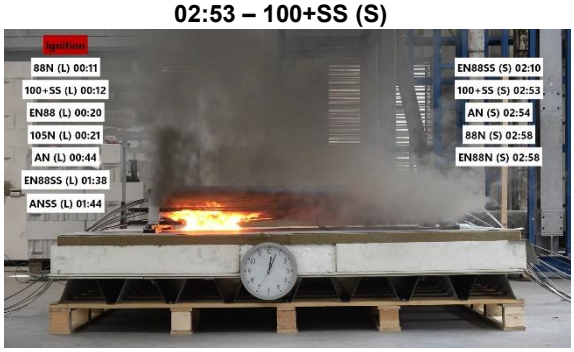

02:58 – EN88N (S)

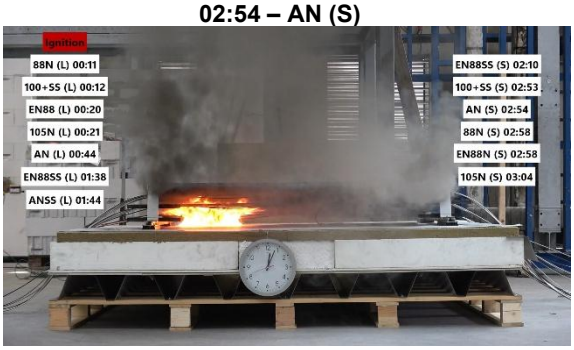

03:04 – 105N (S)

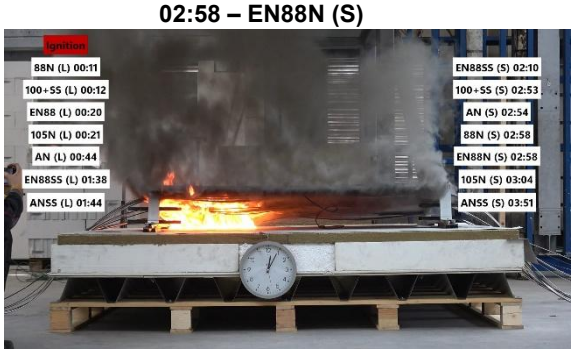

03:51 – ANSS (S)

Figure 18 Snapshots from the camera pointed toward the long edge of the specimen (white boxes show type of LHD cables and their detection times). Times are given in min:s. (FotoPortal from 050522d-004 to 050522d-016)

0:11 – 88N (L)

0:12 – 100+SS (L)

0:20 – EN88 (L)

0:21 – 105N (L)

0:44- AN (L)

01:38 – EN88SS (L)

01:44 – ANSS (L)

02:10 – EN88SS (S)

02:53 – 100+SS (S)

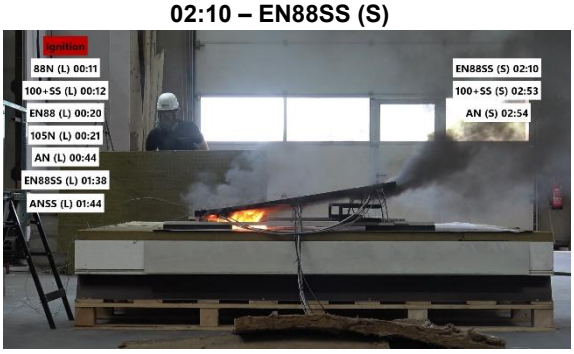

02:54 – AN (S)

02:58 – EN88N (S)

03:04 – 105N (S)

03:51 – ANSS (S)

Figure 19 Snapshots from the camera pointed toward the short edge of the specimen (white boxes show type of LHD cables and their detection times). Times are given in min:s. (FotoPortal from 050522d-017 to 050522d-029)

3.1.2 LHD-2

Date and time of test: 2025.06.16, 10:04.

Temperature/Relative humidity: 17 °C / 41%.

The documented observations and events of the LHD-2 test are summarised in Table 4. The most important events are illustrated by photos and video screenshots taken at times during the test when the detection system was triggered.

Table 4 Observations for test LHD-2

Time (min)	Events
3	Arc generation stopped
2-4	Flames went out from the top and right sides. Delamination of PV cells was observed
4.5	Noticed that cables produce burning droplets
5	Detection cable located at the top edge released volatile compounds that ignited, creating a »jet flame« effect. Flames were coloured blue and green due to the presence of specific chemical components in the LHD cable.
6-7	Fire reached the end of the left side of the specimen
9	Fire slows down. The glass of the PV panel broke.
20	The flames are only around the plastic footing of the mounting system.
21	The last flames were extinguished with water.

Arc generation was stopped in the 3rd minute of the test, around the same time as flames emerged from the top and right side of the PV module, accompanied by visible delamination of solar cells. By minute 4.5, burning droplets were observed dripping from the cables. At 5 min, the detection cable near the top edge emitted volatile compounds, again creating a jet flame effect with blue and green hues (Figure 20).

Around 6-7 minutes into the test, the fire reached the far-left edge of the specimen. By minute 9, the fire actively started to subside, and the glass of the PV panel shattered. Shortly after, the flames confined to the polymeric footing of the mounting system and roofing membrane (Figure 21).

Figure 20 PV module engulfed in flame, along with blue flames coming from the cables (top right corner) (FotoPortal 050522d-030)

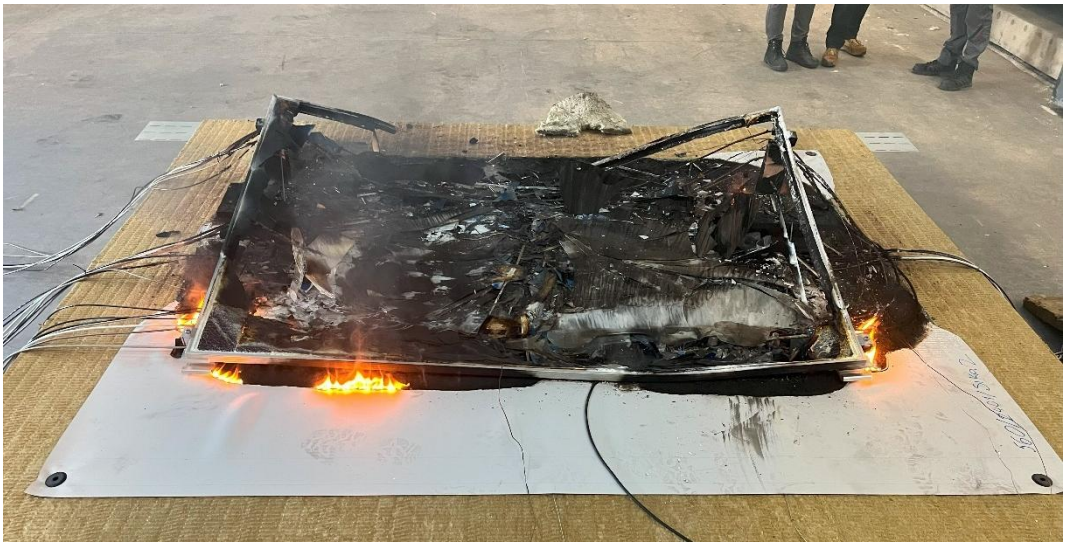

Figure 21 Shattered PV panel and flame residues on the roofing membrane (FotoPortal 050522d-031)

0:37 – 100+SS (L)

0:41 – EN88SS (L)

0:45 – 88N (L)

0:49 – EN88 (L)

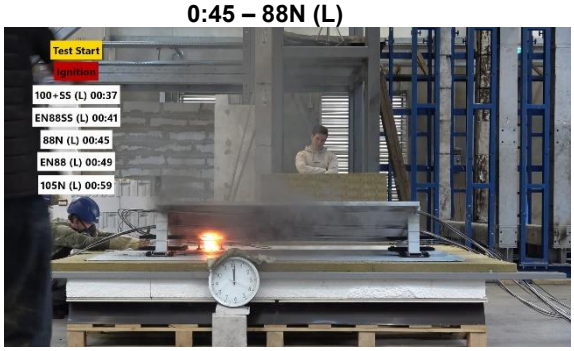

0:59 – 105N (L)

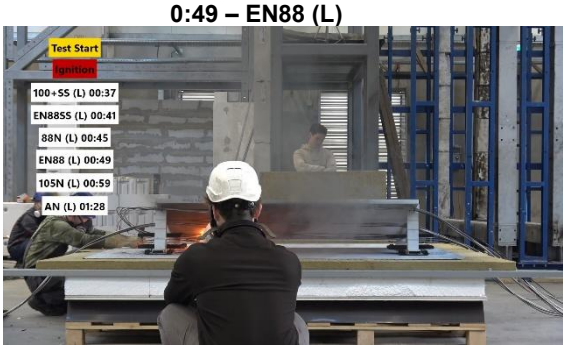

01:28 – AN (L)

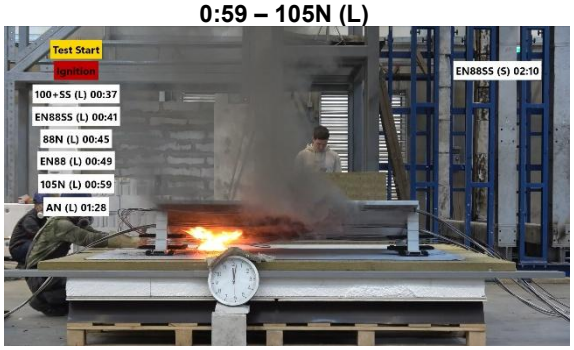

02:10 – EN88SS (S)

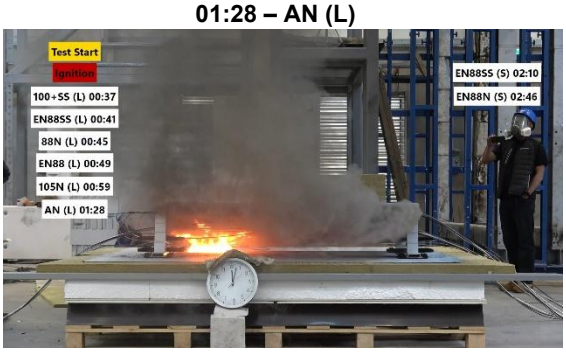

02:46 – EN88N (S)

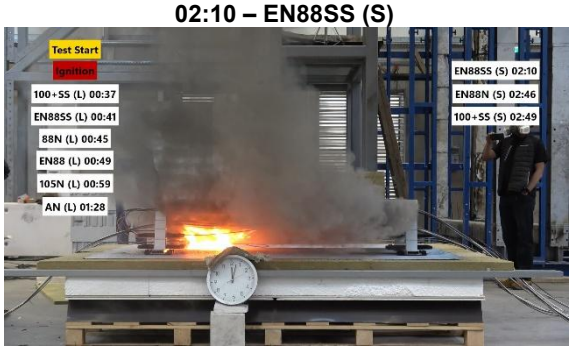

02:49 – 100+SS (S)

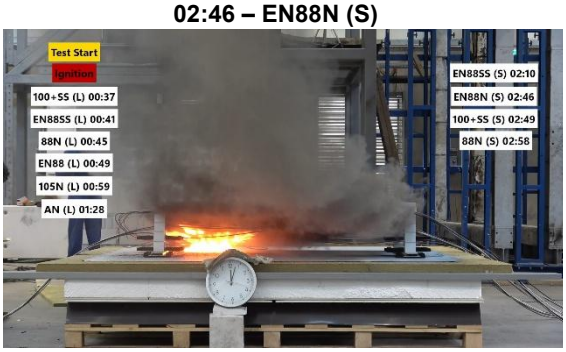

02:58 – 88N (S)

03:00 – 105N (S)

03:08 – AN (S)

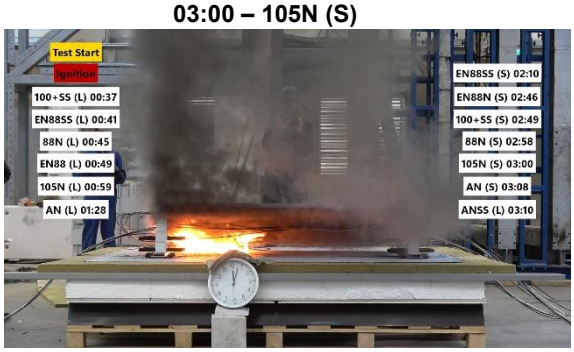

03:10 – ANSS (L)

Figure 22 Snapshots from the camera pointed toward the long edge of the specimen (white boxes show the type of LHD cables and their detection times). Times are given in min:s. (FotoPortal from 050522d-032 to 050522d-044)

0:37 – 100+SS (L)

0:41 – EN88SS (L)

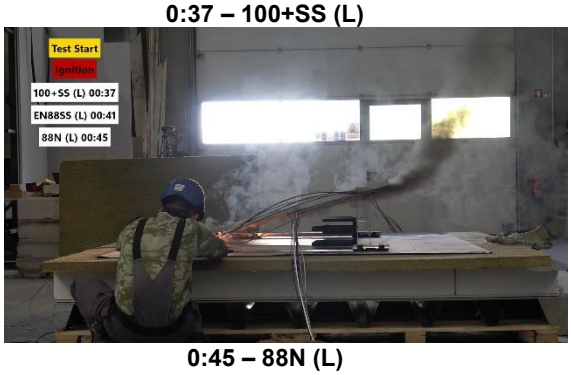

0:45 – 88N (L)

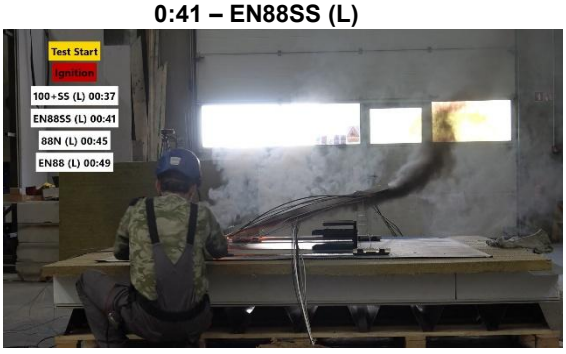

0:49 – EN88 (L)

0:59 – 105N (L)

01:28 – AN (L)

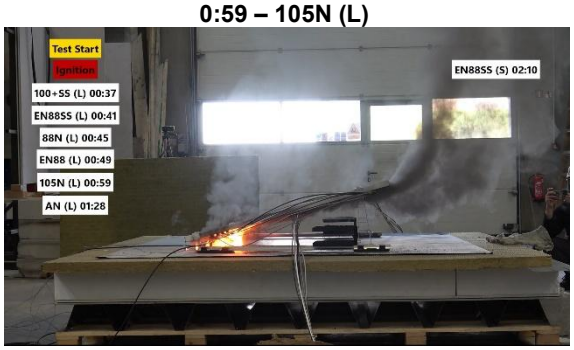

02:10 – EN88SS (S)

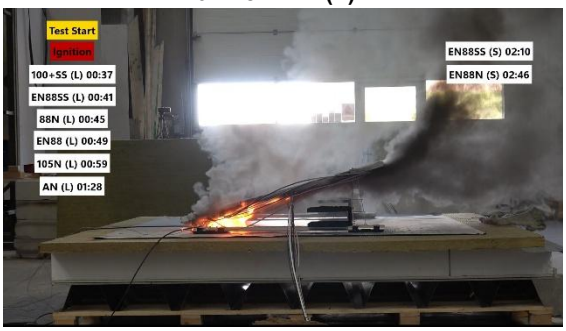

02:46 – EN88N (S)

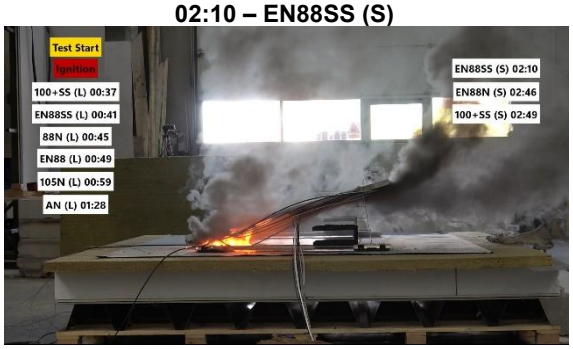

02:49 – 100+SS (S)

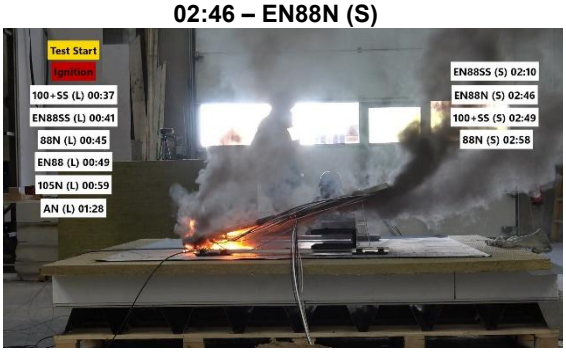

02:58 – 88N (S)

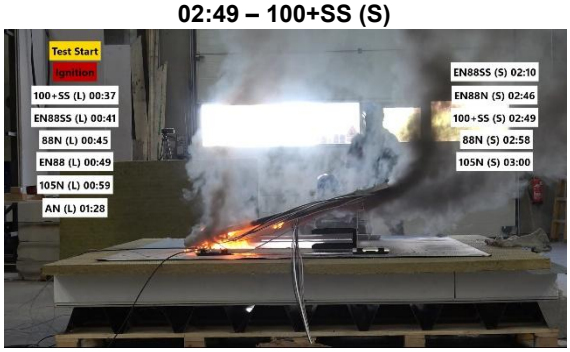

03:00 – 105N (S)

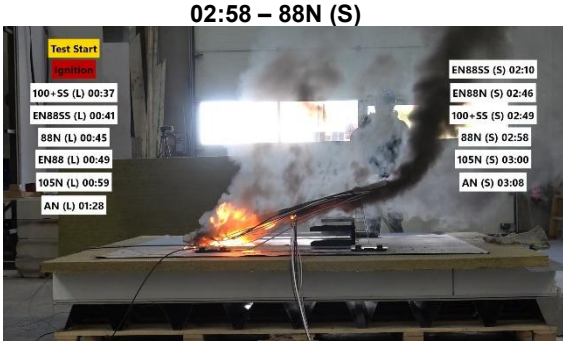

03:08 – AN (S)

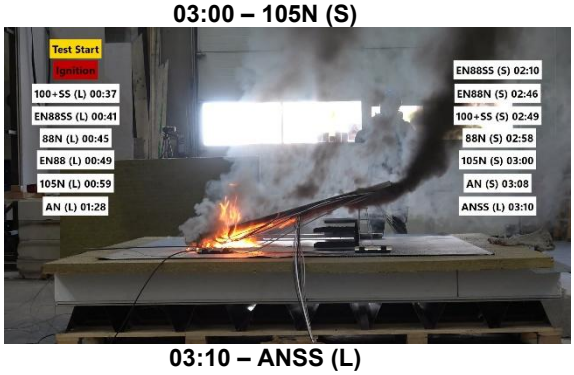

03:10 – ANSS (L)

Figure 23 Snapshots from the camera pointed toward the short edge of the specimen (white boxes show the type of LHD cables and their detection times). Times are given in min:s. (FotoPortal from 050522d-045 to 050522d-057)

3.1.3 LHD-3

Date and time of test: 2025.06.15, 17:16.

Temperature/Relative humidity: 17 °C / 41%.

The documented observations and events of the LHD-3 test are summarised in Table 5. The most important events are illustrated by photos and screenshots from the videos taken at times during the test when a specific sensor of the detection system was triggered.

Table 5 Observations for test LHD-3

Time (min)	Events
2	Arc generation stopped
4	Flames propagated to the top of the PV module
6	Four cells delaminated.
11	The glass of the PV panel broke.
13	The top aluminium edge of the PV broke in the middle, melted.
16	Fire reached the end of the left side of the specimen
25	Fire slows down
30	The test stopped. Small flames were extinguished.

Arc generation stopped after 2 minutes (Figure 24). Shortly after, flames spread upwards and reached the top edge of the PV module by minute 4. At 6 minutes, delamination of solar cells was observed (Figure 25), followed by breakage of the PV glass at minute 11. Two minutes later, the top aluminium edge of the module broke at the centre and began to melt.

By minute 16, flames have reached the far-left end of the specimen. Fire intensity gradually decreased after 25 min, and the test was concluded at minute 30, with only small flames remaining, which were extinguished manually.

Figure 24 The extent of fire on the specimen just after stopping arc generation at 2 min (FotoPortal 050522d-058)

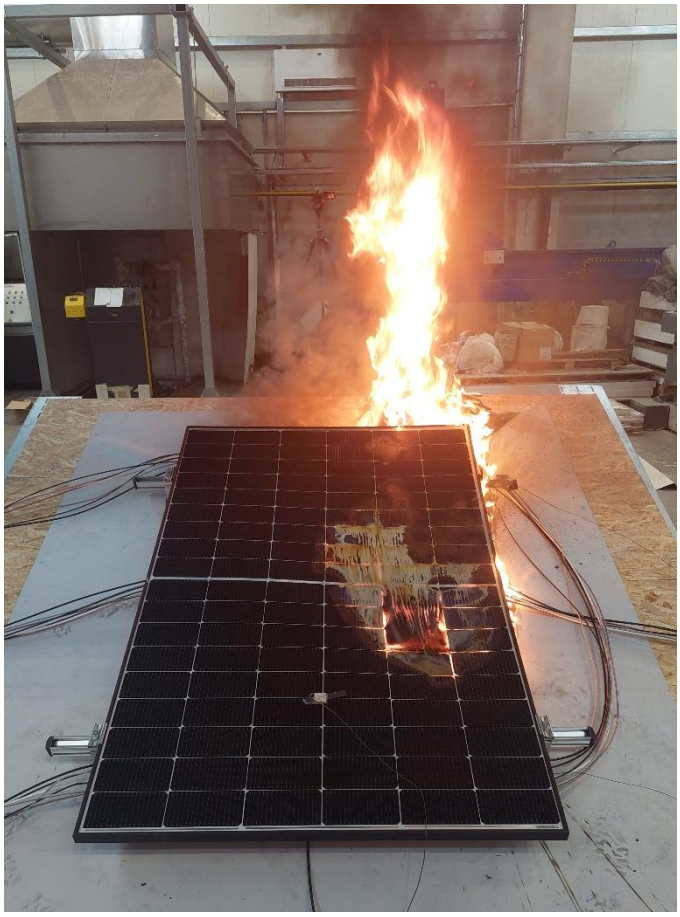

Figure 25 Delamination of solar cells and flame propagation over the top of the PV panel (FotoPortal 050522d-059)

01:47 – EN88N (S)

01:49 – 88N (S)

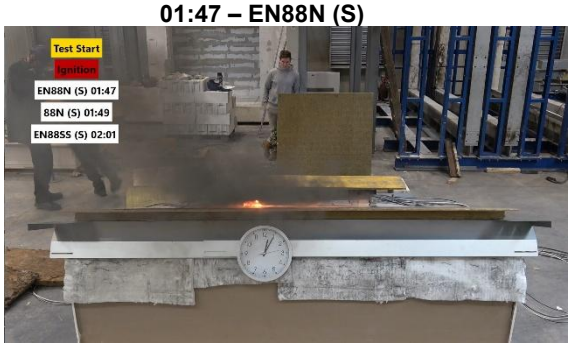

02:01 – EN88SS (S)

02:03 – 100+SS (S)

02:06 – 105N (S)

02:29 – AN (L)

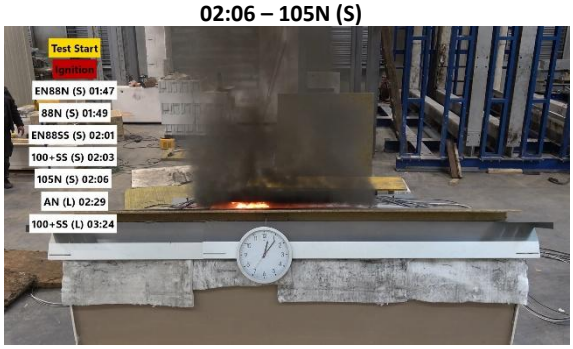

03:24 – 100+SS (L)

03:25 – AN (S)

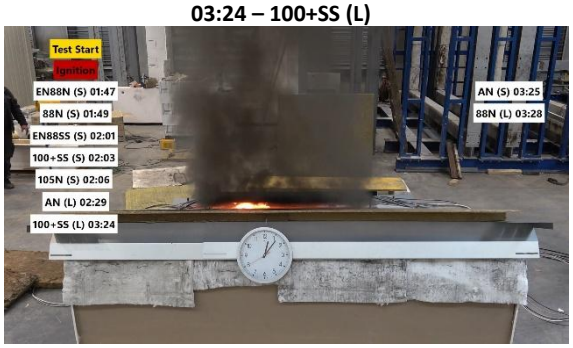

03:28 – 88N (L)

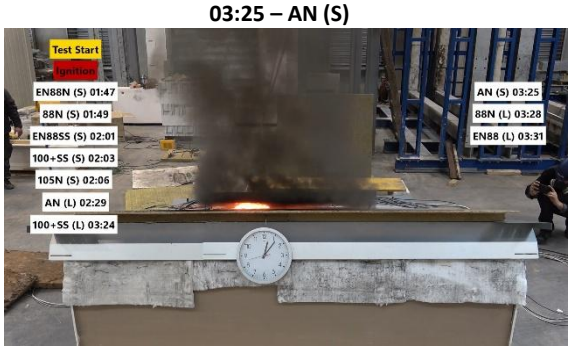

03:31 – EN88 (L)

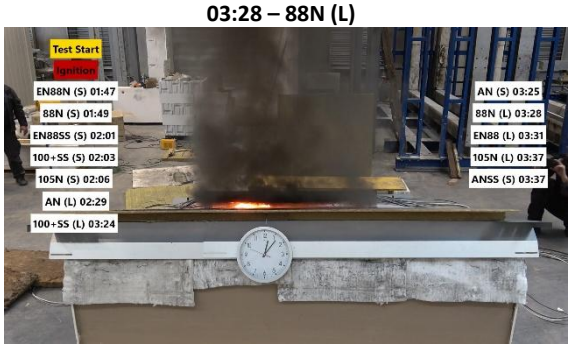

03:37 – ANSS (S)

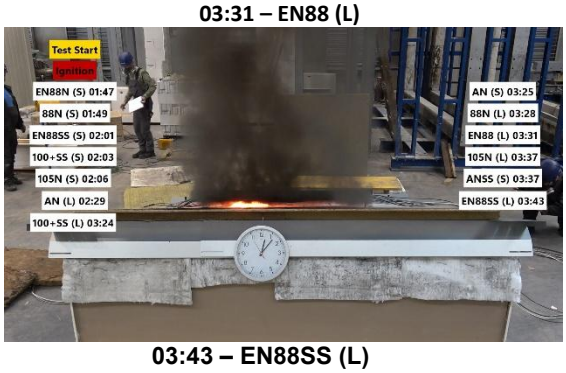

03:43 – EN88SS (L)

Figure 26 Snapshots from the camera pointed toward the long edge of the specimen (white boxes show the type of LHD cables and their detection times). Times are given in min:s. (FotoPortal from 050522d-060 to 050522d-071)

01:47 – EN88N (S)

01:49 – 88N (S)

02:01 – EN88SS (S)

02:03 – 100+SS (S)

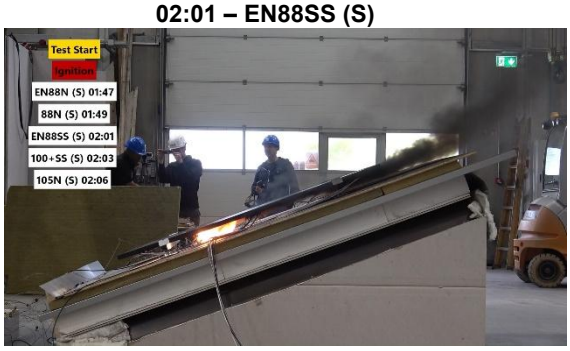

02:06 – 105N (S)

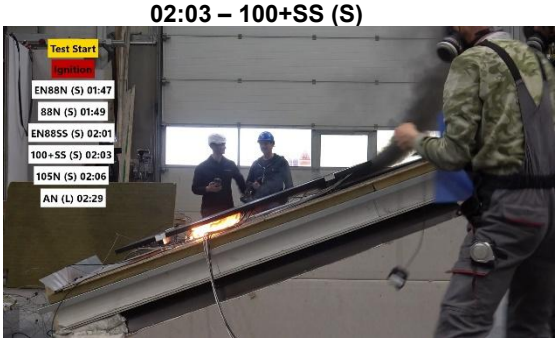

02:29 – AN (L)

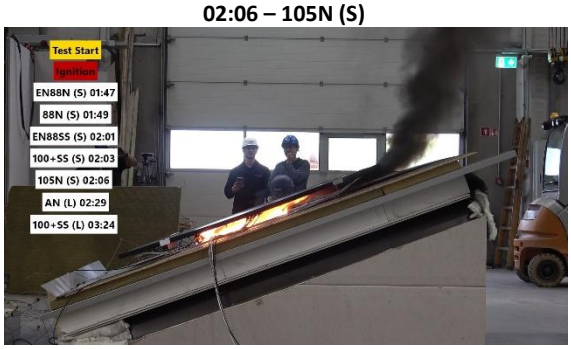

03:24 – 100+SS (L)

03:25 – AN (S)

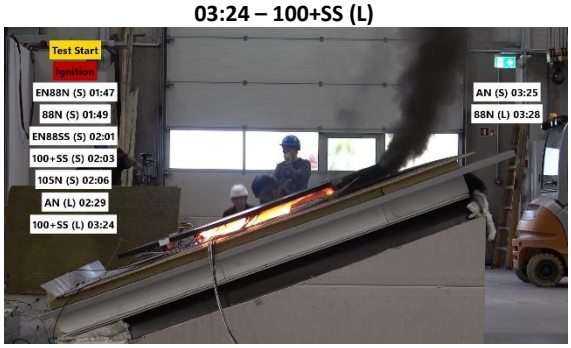

03:28 – 88N (L)

03:31 – EN88 (L)

03:37 – ANSS (S)

03:43 – EN88SS (L)

Figure 27 Snapshots from the camera pointed toward the short edge of the specimen (white boxes show the type of LHD cables and their detection times). Times are given in min:s. (FotoPortal from 050522d-072 to 050522d-083)

3.1.4 LHD-4

Date and time of test: 2025.06.16, 16:20.

Temperature/Relative humidity: 18 °C / 40%.

The documented observations and events of the LHD-4 test are summarised in Table 6. The most important events are illustrated by photos and video screenshots taken at times during the test when the detection system was triggered.

Table 6 Observations for test LHD-4

Time (min)	Events
3	Arc generation stopped
5	Flames went out from the right edge of the 1st PV module
6	Flames went out from the top edge of the 1st PV module.
6.5	Burning droplets from the wires were noticed
8	Flames reached the 3rd and 4th PV modules intersection
9	Fire started to propagate under the 3rd PV module
10	Fire propagated under the 4th PV module
12	The fire was extinguished due to safety reasons. End of the test.

Arc generation stopped after 3 minutes. By minute 5, flames had emerged from the right edge of the first PV module, and shortly after, at minute 6, from its top edge as well (Figure 28). Around minute 6.5, burning droplets falling from the wires were observed. At minute 8, the fire reached the intersection between the third and fourth PV modules, then spread beneath the third module by minute 9 and continued under the fourth by minute 10 (Figure 29).

For safety reasons, the fire was extinguished at minute 12, marking the end of the test.

Figure 28 Flame spread over LHD system after 5-6 min: front (left) and side (right) view (FotoPortal (left 050522d-084, right 050522d-085))

Figure 29 Flame spread over the first PV module (left) and towards the third and fourth modules (right), 8 minutes after ignition (FotoPortal (left 050522d-086, right 050522d-087))

03:34 – Q1 EN88SS

04:22 – Q1 100+SS

04:50 – Q1 AN

07:02 – Q3 EN88SS

07:03 – Q3 100+SS

07:10 – Q2 100+SS

07:16 – Q2 EN88SS

07:17 – Q2 AN

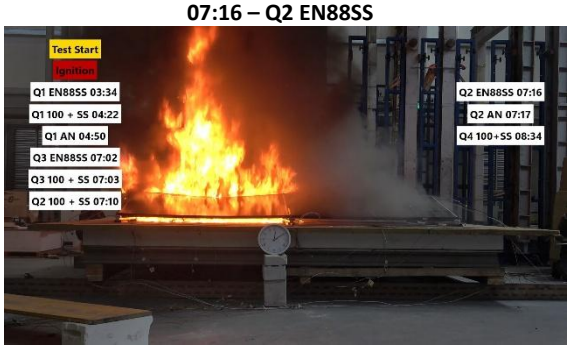

08:34 – Q4 100+SS

08:35 – Q4 AN

08:42 – Q4 EN88SS

Figure 30 Snapshots from the camera pointed toward the long edge of the specimen (white boxes show the type of LHD cables and their detection times). Times are given in min:s. (FotoPortal from 050522d-088 to 050522d-098)

03:34 – Q1 EN88SS

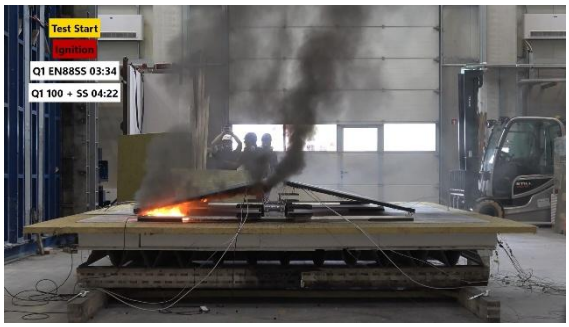

04:22 – Q1 100+SS

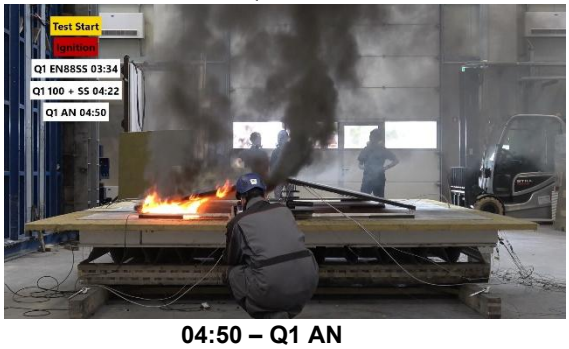

04:50 – Q1 AN

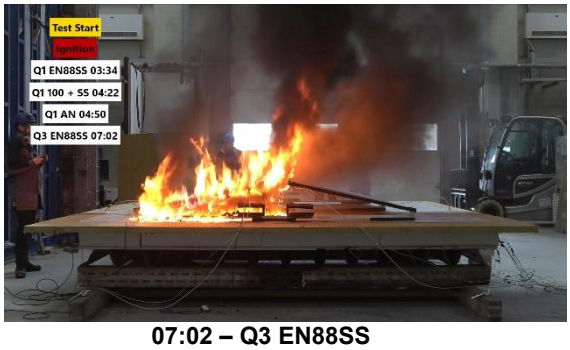

07:02 – Q3 EN88SS

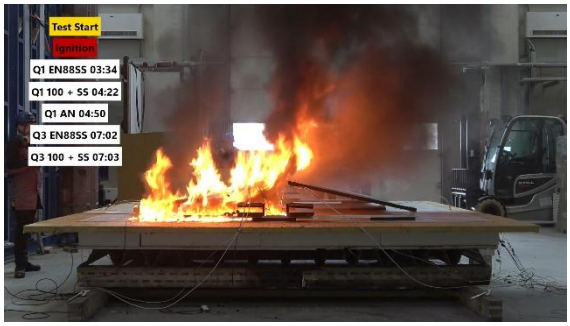

07:03 – Q3 100+SS

07:10 – Q2 100+SS

07:16 – Q2 EN88SS

07:17 – Q2 AN

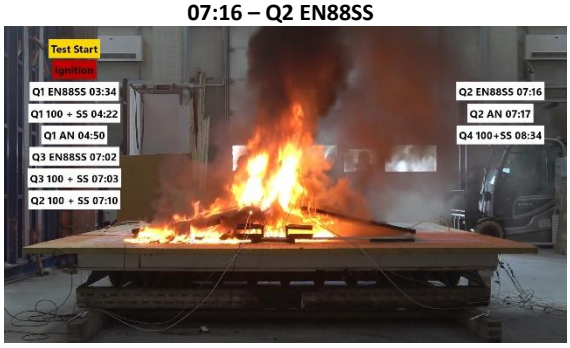

08:34 – Q4 100+SS

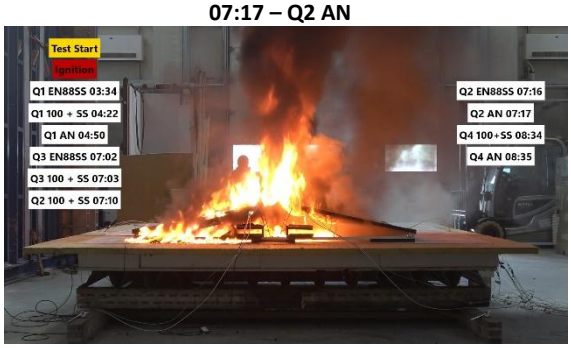

08:35 – Q4 AN

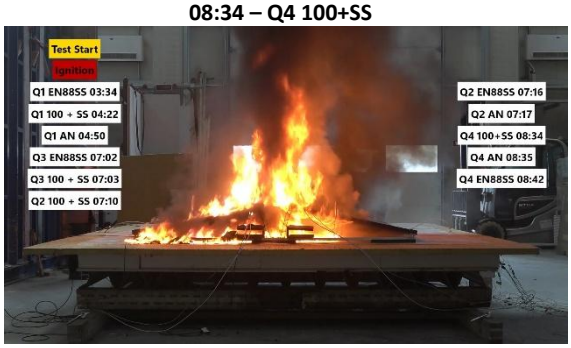

08:42 – Q4 EN88SS

Figure 31 Snapshots from the camera pointed toward the short edge of the specimen (white boxes show the type of LHD cables and their detection times). Times are given in min:s. (FotoPortal from 050522d-099 to 050522d-109)

3.1.5 Aerial perspective

This section presents aerial images of the test setup. These visuals complement the ground-level camera observations by offering a broader spatial overview of fire development and the positioning of the LHD cables. Aerial footage is included for LHD-1, LHD-3, and LHD-4 and presented in Figure 32, Figure 33 and Figure 34, respectively. Due to limitations during data collection, aerial material for LHD-2 is not available.

00:11 – 88N (L)

00:12 – 100+SS (L)

00:20 – EN88 (L)

00:21 – 105N (L)

00:44 – AN (L)

01:38 – AN88SS (L)

01:44 – ANSS (L)

02:10 – EN88SS (S)

02:53 – 100+SS (S)

02:54 – AN (S)

02:58 – 88N (S)

02:58 – EN88N (S)

03:04 – 105N (S)

03:51 – ANSS (S)

Figure 32 Aerial camera snapshots of LHD-1 during alarm activation (white boxes show the type of LHD cables and their detection times). Times are given in min:s. (FotoPortal from 050522d-110 to 050522d-123)

01:47 – EN88N (S)

01:49 – 88N (S)

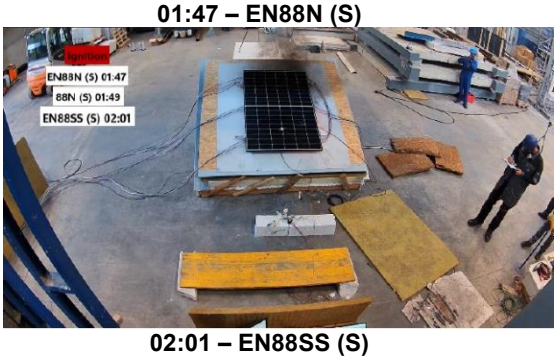

02:01 – EN88SS (S)

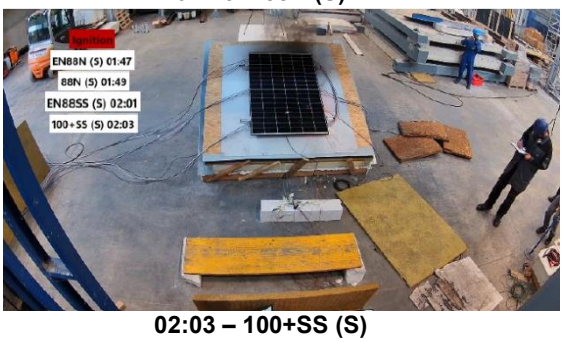

02:03 – 100+SS (S)

02:06 – 105N (S)

02:29 – AN (L)

03:24 – 100+SS (L)

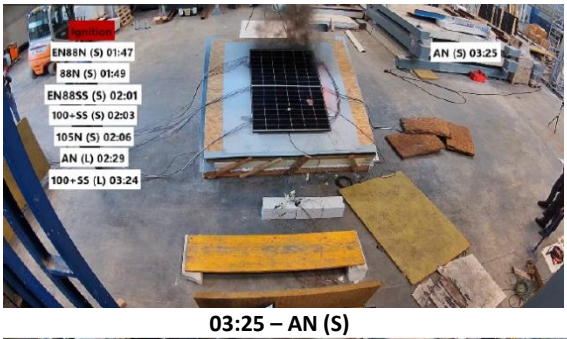

03:25 – AN (S)

03:28 – 88N (L)

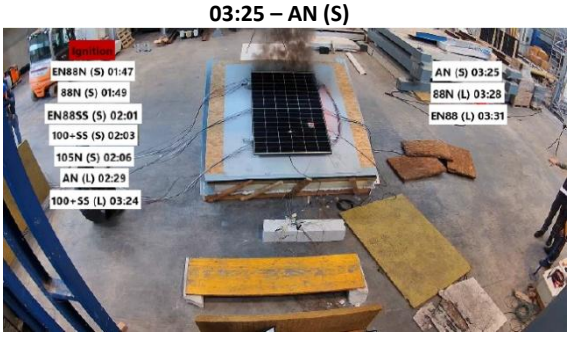

03:31 – EN88 (L)

03:37 – 105N (L)

03:37 – ANSS (S)

03:43 – EN88SS (L)

N/A – ANSS (L)

Figure 33 Aerial camera snapshots of LHD-3 during alarm activation (white boxes show the type of LHD cables and their detection times). Times are given in min:s. (FotoPortal from 050522d-124 to 050522d-137)

03:34 - Q1 EN88SS

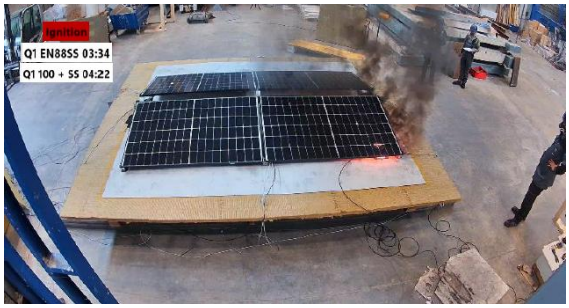

04:22 – Q1 100+SS

04:50 – Q1 AN

07:02 – Q3 EN88SS

07:03 – Q3 100+SS

07:10 – Q2 100+SS

07:16 – Q2 EN88SS

07:17 – Q2 AN

08:34 – Q4 100+SS

08:35 – Q4 AN

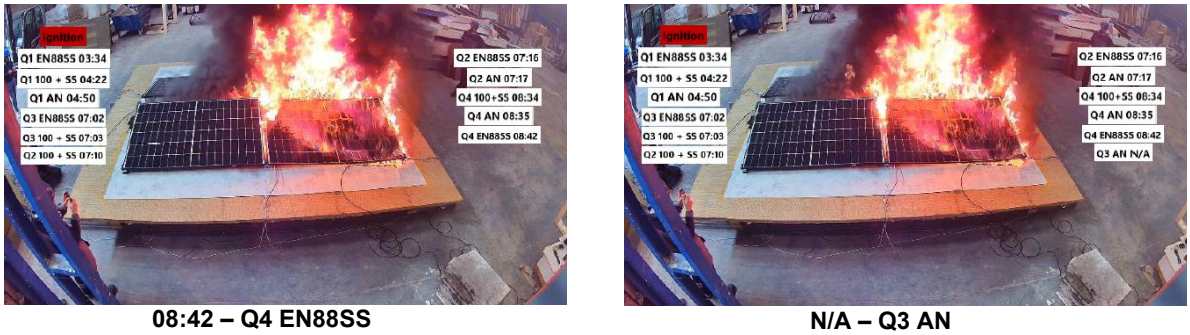

08:42 – Q4 EN88SS **N/A – Q3 AN**

Figure 34 Aerial camera snapshots of LHD-4 during alarm activation (white boxes show the type of LHD cables and their detection times). Times are given in min:s. (FotoPortal from 050522d-138 to 050522d-149)

3.2 Temperature data

The temperature diagrams show the temperature distribution measured on a specific roof layer and on/under PV modules. The numeration of TCs in the temperature graphs correlates with the TC numerations on Figure 8, Figure 10 and Figure 13 for mid-scale, pitched mid-scale and large-scale roofs, respectively. The cooling phase was not recorded. Malfunctioned TCs were excluded from the graphs if they failed completely. However, some TCs that showed irregularities only during part of the measurement were retained, as the errors were limited in scope and the overall trends can still be envisioned.

3.2.1 LHD-1

Figure 35 shows the temperature distribution across all layers during the LHD-1 test. Each layer is represented by a single colour, using a solid and a dashed line for the two distinct TCs. Thermocouples 7 and 8 are located within the PV module.

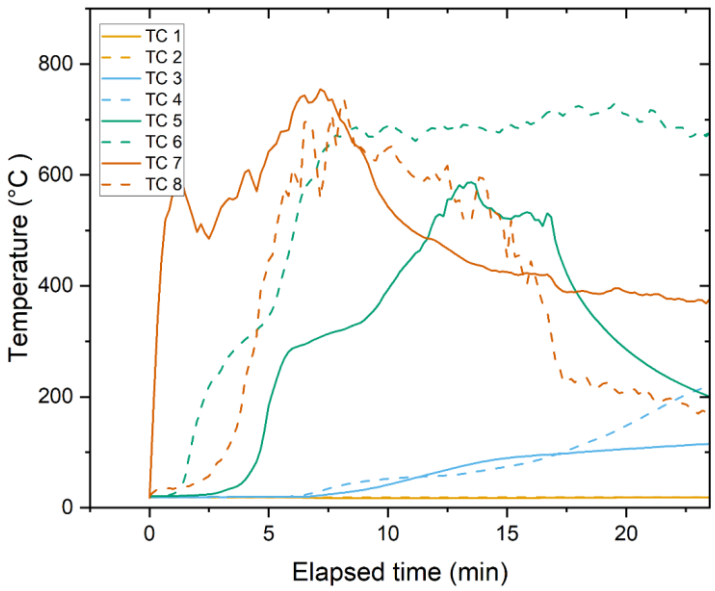

Figure 35 Temperature distribution on all layers (colour represents one layer, full or dashed line represents a TC location)

3.2.2 LHD-2

Figure 36 shows the temperature distribution across all layers during the LHD-2 test. Each layer is represented by a single colour, using a solid and a dashed line for the two distinct TCs. Thermocouples 7 and 8 are located within the PV module.

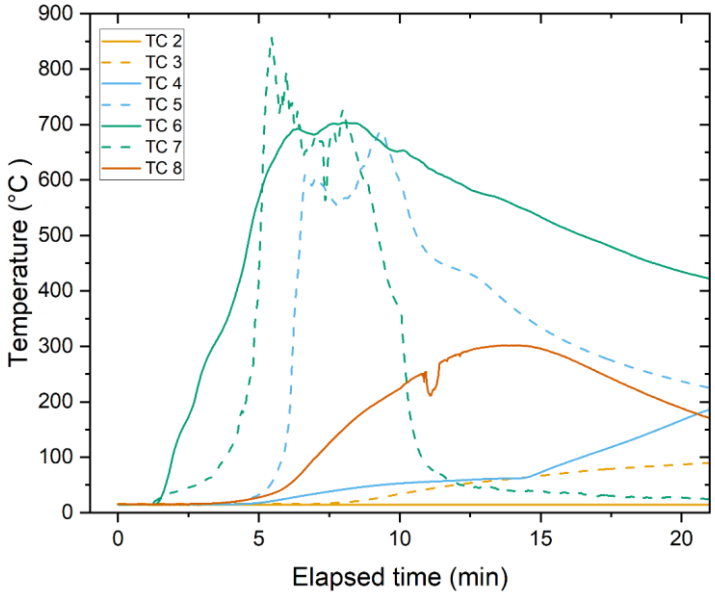

Figure 36 Temperature distribution on all layers (colour represents one layer, full or dashed line represents a TC location)

3.2.3 LHD-3

Temperature distributions during the LHD-3 test are presented in Figure 37, Figure 38, Figure 39, and Figure 40. Each figure shows a different roof layer, with thermocouples split across multiple graphs due to their large number. Figure 40 specifically displays TCs installed on the PV module.

In Figure 39 TC14 shows a higher baseline temperature than the other thermocouples - approximately 50 °C. This was related to a failed ignition attempt before the test, during which the arc connectors melted. Although ignition did not occur, some localised heating was generated, and TC14, being positioned directly beneath the arc, recorded elevated temperatures as a result.

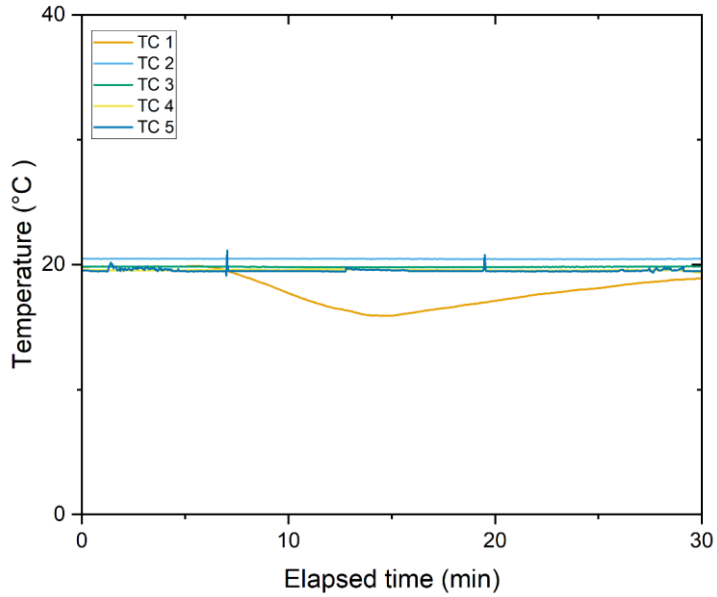

Figure 37 Temperature distribution under insulation

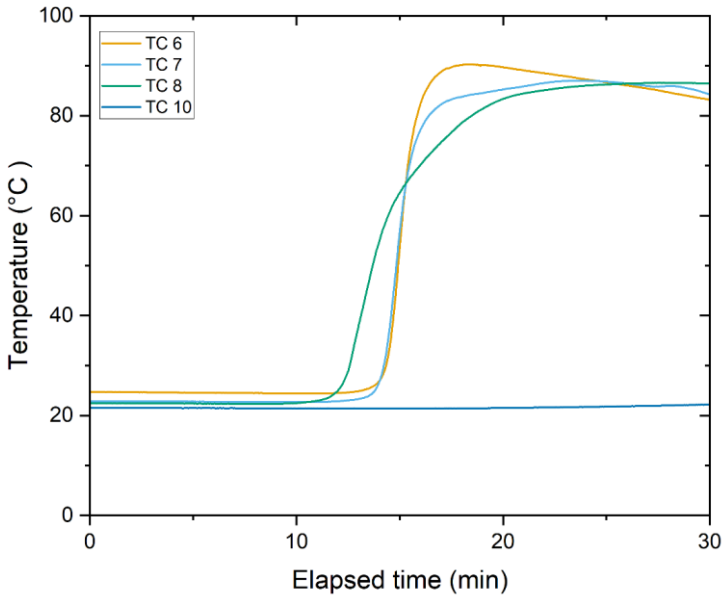

Figure 38 Temperature distribution on insulation

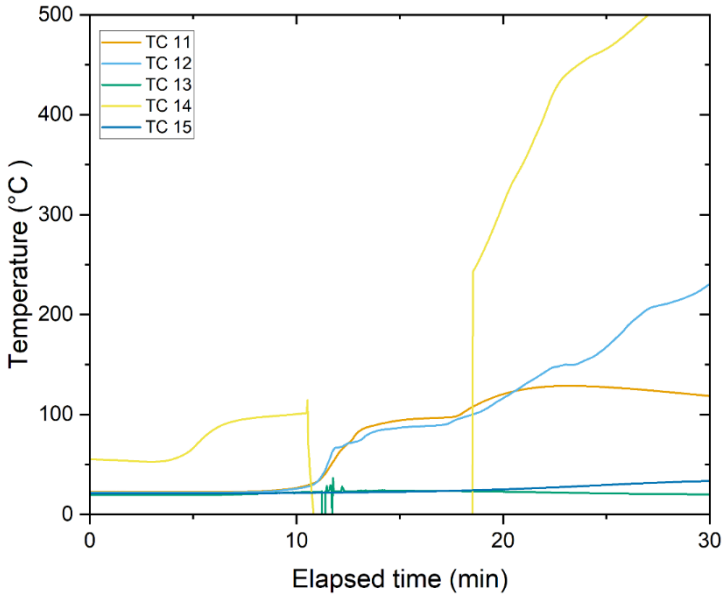

Figure 39 Temperature distribution on mineral wool

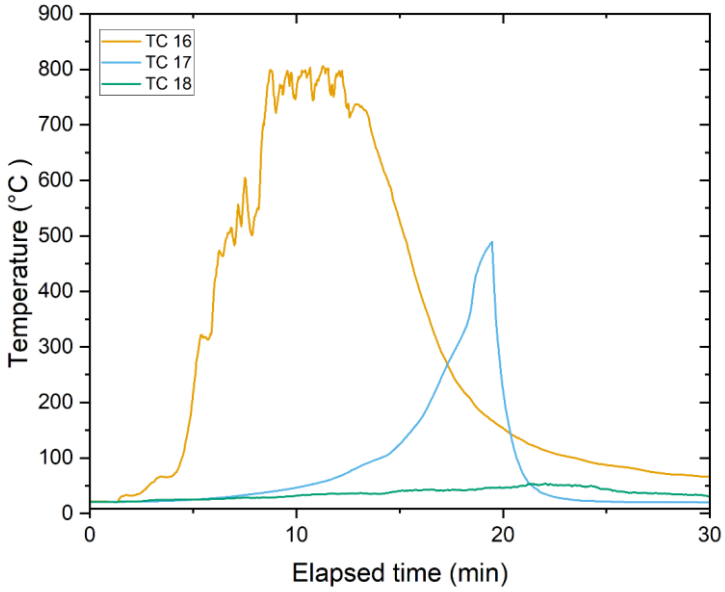

Figure 40 Temperature distribution on the PV module

3.2.4 LHD-4

Temperature distributions during the LHD-4 test are presented in Figure 41, Figure 42, Figure 43, and Figure 44. Each figure shows a different roof layer, with thermocouples split across multiple graphs due to their large number. Figure 44 specifically displays TCs installed on the PV module.

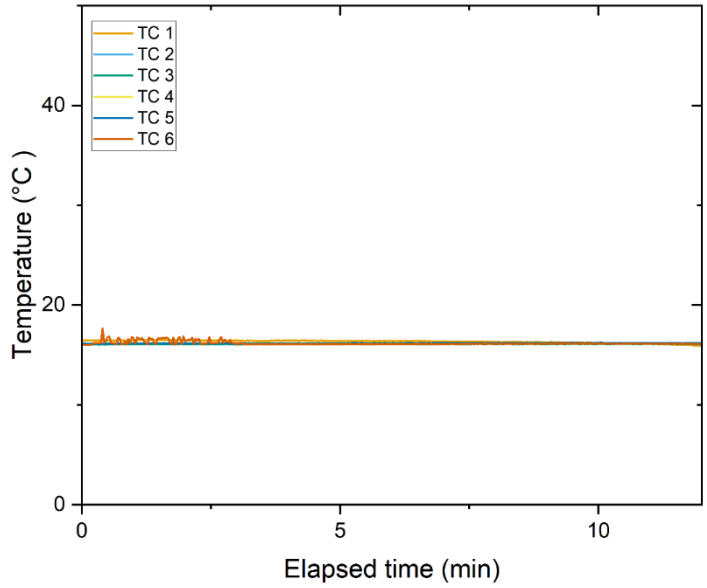

Figure 41 Temperature distribution under insulation

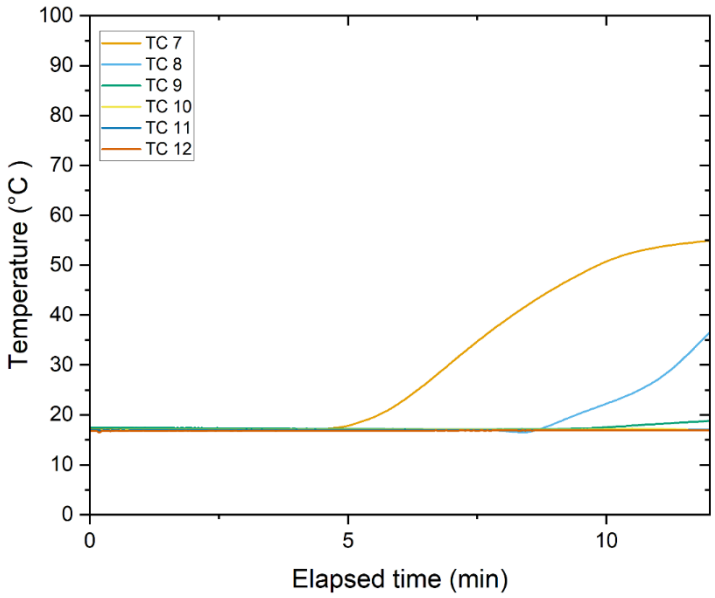

Figure 42 Temperature distribution on insulation

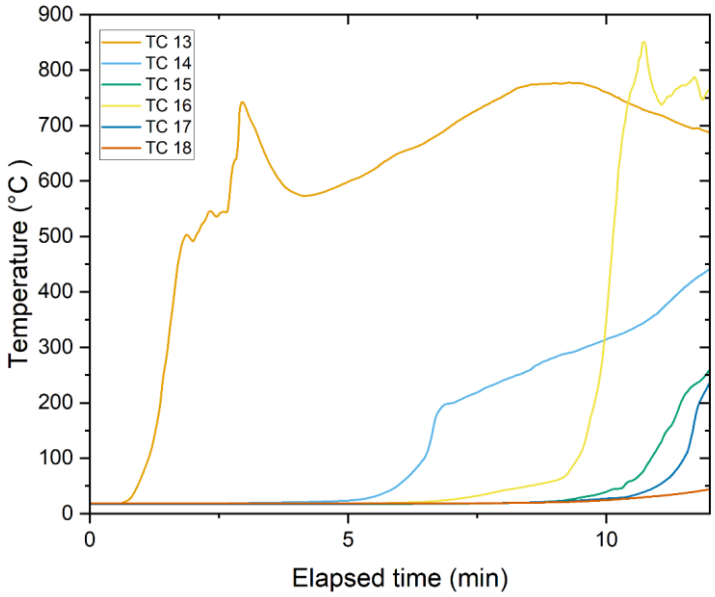

Figure 43 Temperature distribution on mineral wool

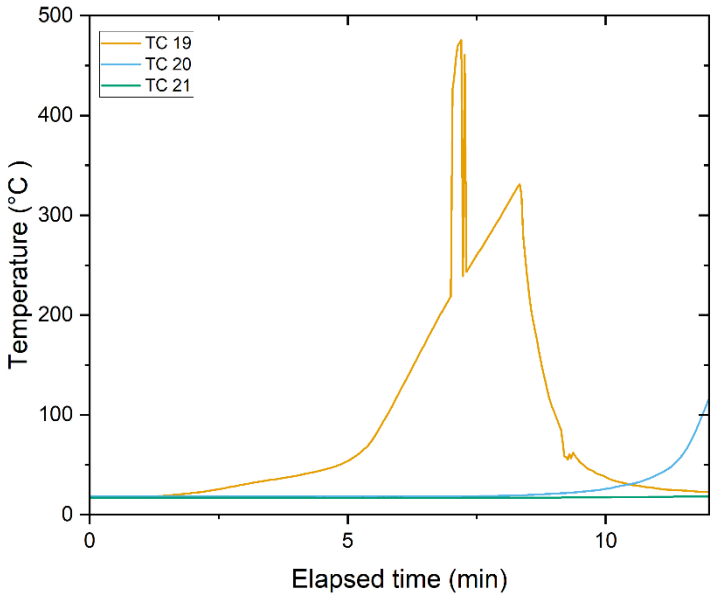

Figure 44 Temperature distribution on the PV module

3.3 LHD alarm times

This section presents an overview of the alarm activation times recorded for each Linear Heat Detection (LHD) cable during the test. By compiling the alarm times in one place, this section allows for a clearer comparison between the different LHD systems and their response to the rise in temperature due to the developing fire conditions. The results are shown in Table 7.

Table 7 LHD alarm times

Cable/ Test	88N		EN88		EN88SS		105N		100+SS		ANSS		AN	
	Long	Short	Long	Short	Long	Short	Long	Short	Long	Short	Long	Short	Long	Short
LHD-1	00:11	02:58	00:20	02:58	01:38	02:10	00:21	03:04	00:12	02:53	01:44	03:51	00:44	02:54
LHD-2	00:45	02:58	00:49	02:46	00:41	02:10	00:59	03:00	00:37	02:49	03:10	ND	01:28	03:08
LHD-3	03:28	01:49	03:31	01:47	03:43	02:01	03:37	02:06	03:24	02:03	ND	03:37	02:29	03:25
LHD-4					**EN88SS**				**100+SS**				**AN**	
Q1					03:43				04:22				04:50	
Q2					07:16				07:10				07:17	
Q3					07:02				07:03				ND	
Q4					08:42				08:34				08:35	

3.4 Correlation between temperatures and times of detection

To better understand the detection times and their relationship to temperature development recorded by the installed TCs, additional graphs have been plotted. These focus on the first 3 to 10 minutes of the experiments, depending on detection time, and show the temperatures recorded by the nearest TCs, both in the roof (uppermost layer) and on the PV modules. All detection cables used in the tests (88N, EN88, EN88SS, 105N, 100+SS, ANSS, and AN) are displayed on the same graphs for comparison.

3.4.1 LHD-1

The temperature development in the vicinity of the detectors during the LHD-1 test is presented in Figure 45. In this test, the earliest activation was registered by the 88N cable in long configuration. Due to the wood crib ignition, rapid flame development led to high temperatures within the first minute, close to 600 °C on the PV module surface. This intense thermal exposure resulted in short alarm times for several cables, particularly those placed closer to the ignition point.

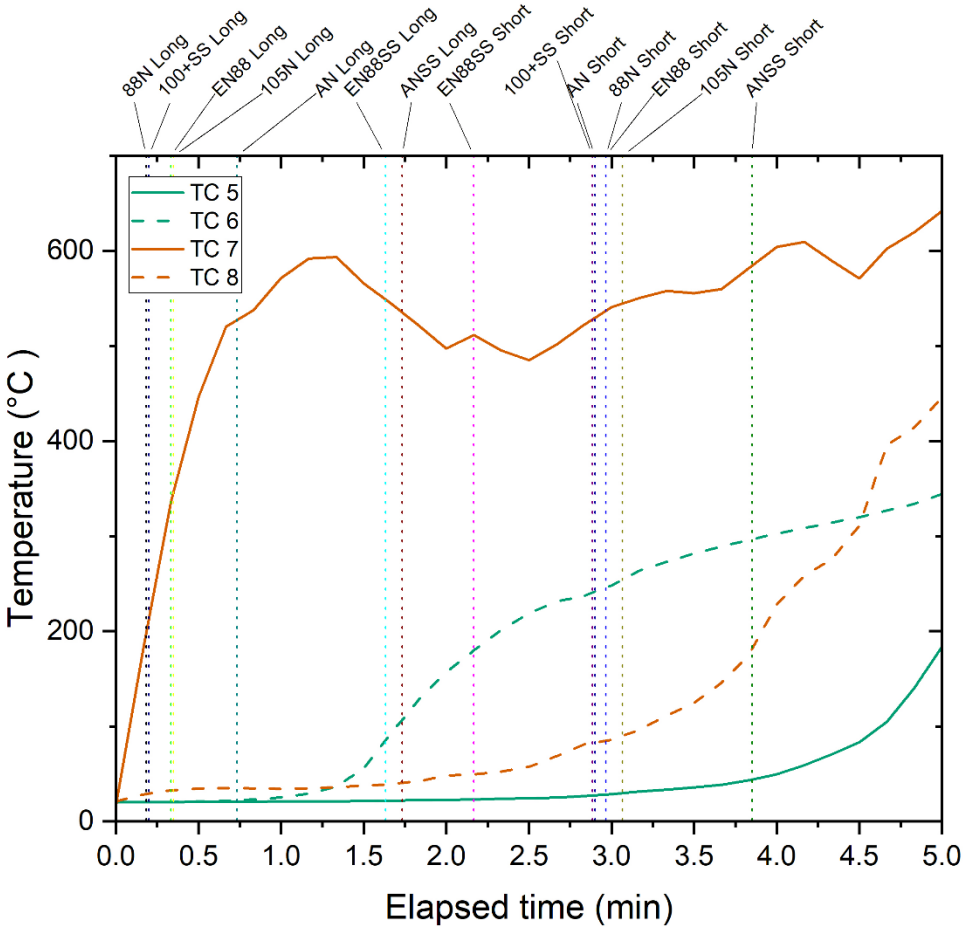

Figure 45 Detection times (vertical dotted lines) and temperatures of the nearest TCs for LHD-1

3.4.2 LHD-2

The temperature development in the vicinity of the detectors during the LHD-2 test is presented in Figure 46. In contrast to LHD-1, the ignition source was an electrical arc, which resulted in a slower and more localised fire development. The earliest detection was recorded by the 100+SS cable in long configuration. Unlike the LHD sensors, the TC instrumentation around the PV module did not detect such a rapid temperature rise, potentially due to the more localised nature of the arc as an ignition source, compared to the wood cribs. The delay and lower thermal exposure highlight the importance of cable sensitivity in less aggressive ignition scenarios.

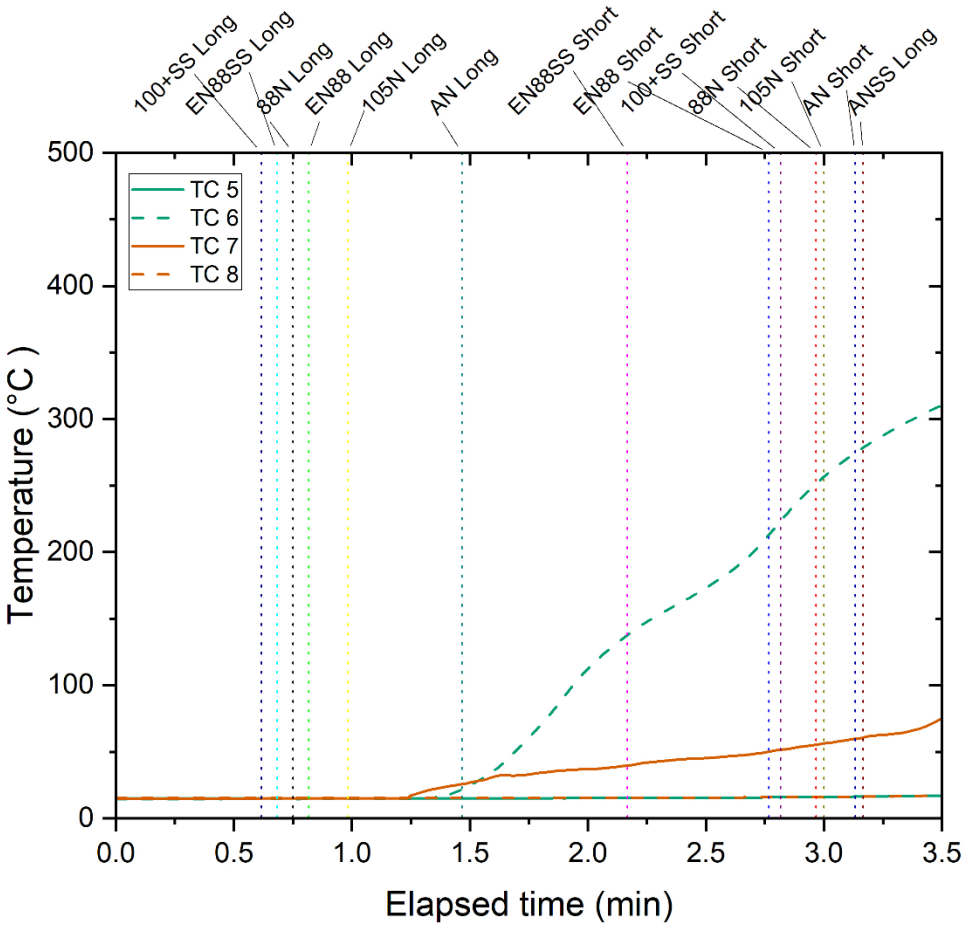

Figure 46 Detection times (vertical dotted lines) and temperatures of the nearest TCs for LHD-2

3.4.3 LHD-3

The temperature development in the vicinity of the detectors during the LHD-3 test is presented in Figure 47. In this test, the earliest activation was registered by the EN88 cable in short configuration. The test setup included a 20° slope, which influenced fire dynamics - hot gases and flames accumulated towards the upper part of the panel, where the short run was positioned. Consequently, detection occurred at low temperatures (around 30°C on the PV module), with some short-run cables triggering alarms earlier than their longer counterparts. This highlights the significant effect of geometry and heat plume movement on detection timing.

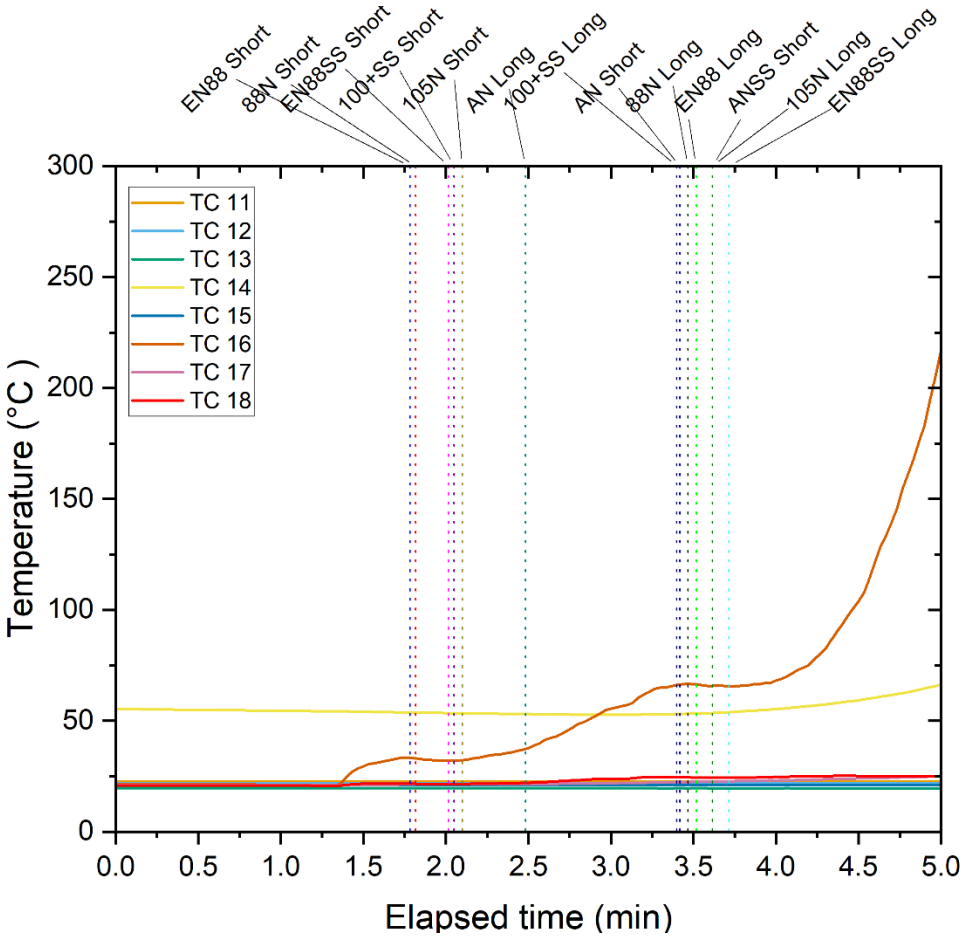

Figure 47 Detection times (dotted lines) and temperatures of the nearest TCs for LHD-3

3.4.4 LHD-4

The temperature development in the vicinity of the detectors during the LHD-4 test is presented in Figure 48. In this test, the earliest activation was registered by the EN88SS cable at Q1, which was located closest to the ignition source. Q1 to Q4 correspond to quadrants – PV modules on the large-scale roof that was tested, depicted in Figure 13. Despite the ignition being similar to previous tests, the fire spread more slowly across the setup due to its size, resulting in later detections and generally lower temperatures at the time of alarm, often below 100 °C. The delay in detection across modules Q2 to Q4 underlines the impact of both cable placement and distance from the ignition source, particularly in large PV installations with multiple zones.

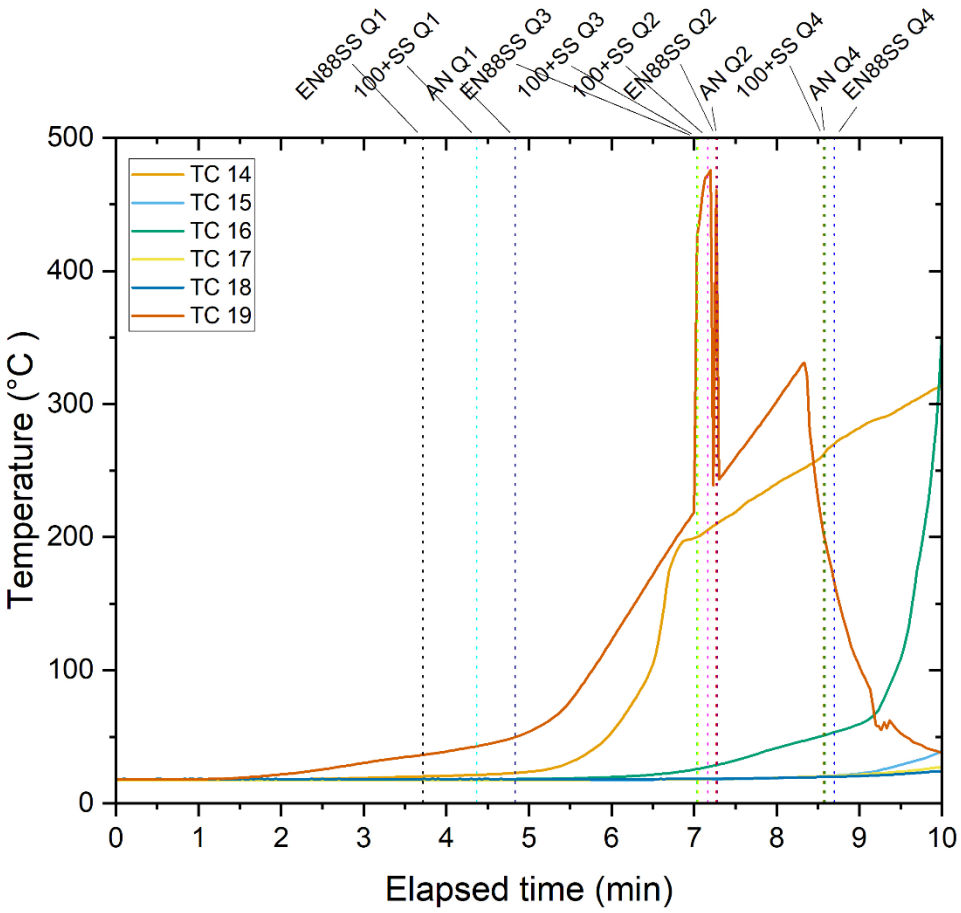

Figure 48 Detection times (dotted lines) and temperatures of the nearest TCs for LHD-4

4. Conclusions

All four fire tests (LHD-1 to LHD-4) demonstrated consistent patterns of fire development beneath and around the PV modules, with notable involvement of the membrane layer, module delamination, and eventual glass breakage. Despite variations in ignition method (wood crib or arc), module geometry, and slope angle, fire typically progressed across the roof within the first 5-10 minutes.

To better understand the link between fire development and detection performance, temperature measurements near the detection cables were analysed. The detection times were then compared across seven different Linear Heat Detection (LHD) systems.

The results confirm that early detection depends on both the installation type of the cables and their position relative to the ignition source. In LHD-1, where ignition occurred directly beneath the long cable run, the 88N triggered an alarm in just 11 seconds, representing the fastest detection observed across all tests. Other cables, such as EN88, 105N, 100+SS, and AN, also responded in under a minute, particularly in the ‘long’ configuration, demonstrating effective early warning on flat roofs under wood crib ignition.

In LHD-2, with arc ignition on a flat roof, similar early detection was observed. The 100+SS responded in 37 seconds, and 88N, EN88, EN88SS, and 105N all detected fire within one minute. This reinforces the finding that flat roof installations with long cable runs placed directly above or near the ignition source enable rapid alarm activation.

In contrast, LHD-3 featured a 20° sloped roof where ignition occurred near the bottom edge. Here, the fastest detection came from short runs positioned in the middle of the slope. EN88, in this configuration, alarmed in 1 minute and 47 seconds. Notably, the relative positions of the long cable runs differed from the flat roof configurations, making direct comparison with LHD-1 and LHD-2 unsound without accounting for the detector placement and heat flow path.

The large-scale arc-ignited test (LHD-4) further illustrates the influence of layout and scale. Response times ranged from 3 minutes and 43 seconds to 8 minutes and 42 seconds. The earliest alarm in this case came from EN88SS installed in quadrant Q1. However, the detector placements varied considerably from the previous setups, further emphasising that spatial configuration and thermal dynamics must be considered before drawing performance comparisons across different test geometries.

In conclusion, effective early warning for PV fires on roofs can be achieved using LHD systems, but the performance is sensitive to installation geometry, fire origin point, roof slope, and cable construction. Future deployment should therefore tailor cable positioning and type to the specific fire dynamics expected in the target configuration.

Prepared by: dr. Andrea Jurov, mag. educ. phys., Kirils Simakovs, MSc., Nik Rus, mag. inž. teh. var.

Reviewed by: Prof. Grunde Jomaas, PhD.

Thermocable

World leading linear detection

About us

Founded in 1963 as a manufacturer of heating cables for the refrigeration and electric blanket markets, Thermocable has continued to innovate and develop, becoming the world leading manufacturer of linear detection cable and monitoring systems.

This transformation has been driven by our boundless desire to problem solve, as well as our fundamental company values, enabling us to supply to multi-disciplinary customers on a global scale.

Recognising our commitment to making the world a safer place, Thermocable was acquired by the renowned FTSE 100 plc, Halma, in February 2023. As a global group of life-saving technology companies, Halma companies strive to grow a safer, cleaner and healthier future for everyone.

Operating within the Apollo Group, we continue to innovate in high quality, certified linear detection products, designed to raise the bar in the industry.

As an ISO 9001:2015 accredited, internationally qualified category solutions provider, Thermocable offers a vertically integrated lean approach through design, development and manufacturing, providing reassurance of a flexible and responsive approach to our customer needs.

Our accreditations

ISO 9001:2015

Approved EN54-28 Approved

UL CERTIFIED SAFETY SIGNALING

VdS

Approved EN54-22 Approved

CE RoHS SIL2

CNBOP-PIB

c UL US LISTED